AD NUMBER

ADB271511

NEW LIMITATION CHANGE

TO

Approved for public release, distribution unlimited

FROM

Distribution: Further dissemination only as directed by or higher DoD authority.

AUTHORITY

DTRA, DTIC Form 55 dtd 18 Oct 2005

# TRANSLATIONAL EFFECTS OF AIR BLAST
# FROM HIGH EXPLOSIVES

I. Gerald Bowen

Paul B. Woodworth

Mary E. Franklin

Clayton S. White, M. D.

Lovelace Foundation for Medical Education and Research

Albuquerque, New Mexico

# CHAPTER 1 INTRODUCTION AND SUMMARY

A portion of the studies of the biological effects of blast from nuclear explosions has been concerned with the translational effects of blast waves for objects as small as a 10-mg stone and as large as a 168-lb man. Computed results from theoretical studies[1,2] when compared to field data for near-ideal blast waves from nuclear explosions[3,4,5] have demonstrated that the motion of experimental objects can be satisfactorily predicted for free-field conditions or for window glass in houses.

This report presents for high explosives (surface burst) the results of a similar theoretical study — specifically, computed velocity, displacement, and acceleration as functions of time for a variety of objects exposed to blast waves with 12 maximum overpressures ranging from 1 to 20 atm. Although all computations were made for 1 ton of high explosives, the results may be readily scaled to lower or higher yields. The translated objects, or missiles, are identified in this study by their acceleration coefficients* which range from 0.01 to 6.0 $ft^2/lb$.**

---

*Acceleration coefficient is defined for an object as its area presented to the wind times its drag coefficient divided by its mass. See Ref. 2.

**This range in acceleration coefficients is for 1 ton of high explosives. Because of scaling laws (see Sect. 2.1), different ranges would apply to other yields.

REFERENCES  CHAPTER 1

1.  Bowen, I. G., R. W. Albright, E. R. Fletcher and C. S. White, A Model Designed to Predict the Motion of Objects Translated by Classical Blast Waves, Civil Effects Test Operations, USAEC Report CEX-58.9, June 29, 1961.

2.  Fletcher, E. R., R. W. Albright, V. C. Goldizen and I. G. Bowen, Determinations of Aerodynamic-Drag Parameters of Small Irregular Objects by Means of Drop Tests, Civil Effects Test Operations, USAEC Report CEX-59.14, October 1961.

3.  Bowen, I. G., A. F. Strehler and M. B. Wetherbe, Distribution and Density of Missiles from Nuclear Explosions, Operation Teapot Report, WT-1168, December 1956.

4.  Bowen, I. G., Mary E. Franklin, E. R. Fletcher and R. W. Albright, Secondary Missiles Generated by Nuclear-Produced Blast Waves, Operation Plumbbob Project 33.2 Report WT-1468, submitted to Mr. L. Joe Deal, Division of Biology and Medicine, U. S. Atomic Energy Commission, on March 7, 1962. (in press)

5.  Taborelli, R. V., I. G. Bowen and E. R. Fletcher, Tertiary Effects of Blast — Displacement, Operation Plumbbob Report, WT-1469, May 22, 1959.

# CHAPTER 2 ANALYTICAL PROCEDURES

## 2.1 THE MODEL

The computational model used in this work was reported in Ref. 1 and will not be described in detail. In the previous study tabular values of computed velocity, displacement, and acceleration as functions of time were presented as nondimensional quantitites for missiles produced by nuclear blast waves. However, to make interpretation of the results easier, the computations in the present study for missiles produced by high-explosive blast waves were made in dimensional form for a yield of 1 ton, and the results are presented graphically. Dimensional analysis derived previously[1] make it possible to apply the results to explosions of lower or higher yields within the limits of weapons' scaling.

In deriving the computational model (see Ref. 1), the following assumptions were made: (1) Friction between the missile (translated object) and the surface was negligible. (2) The effect of gravity on the horizontal velocity of the missile could be neglected. (3) Only the winds associated with the blast wave contributed to missile translation. (4) The acceleration coefficient of the missile could be assumed to be constant. (5) The blast wave does not decay appreciably while passing the missile.

Allowance was made for the object's being exposed to the blast winds for a time dependent on the relative velocity of the missile and the blast wave. This effect was particularly important for the missiles with the higher acceleration coefficients which are propelled to relatively high velocities.

Numerical solutions of the model were determined by stepwise integration of the model equations.[1] For missile velocity, the following was used

$$\pm \Delta v = e + f - \sqrt{e^2 + f^2 + 2 f g} \tag{1}$$

where

$\Delta v$ is positive if $u_o > v_o$,

$\Delta v$ is negative if $u_o < v_o$,

$\Delta v$ = change in missile velocity during time step $\Delta t$,

$e = \underline{\dot{x}} - v_o$,

$$f = \alpha\, \underline{q}\, (\underline{u} - v_o)\, \underline{\dot{x}}\, \Delta t / \underline{u}^2,$$

$$g = \underline{\dot{x}} - \underline{u},$$

$u_o$ = wind velocity at beginning of $\Delta t$,

$v_o$ = missile velocity at beginning of $\Delta t$,

$\underline{u}$ = average wind velocity during $\Delta t$,

$\underline{\dot{x}}$ = average velocity of propagation of blast wave during $\Delta t$, approximated by $\underline{\dot{x}} = 0.6\, \underline{u} + \sqrt{c_o^2 + .36\, \underline{u}^2}$

$c_o$ = velocity of sound in the undisturbed air

$\alpha$ = acceleration coefficient = $s\, C_d / m$,

$s$ = area presented to wind by missile,

$C_d$ = drag coefficient of missile,

$m$ = mass of missile, and

$\underline{q}$ = average dynamic pressure during $\Delta t$.

Incremental distance, $\Delta d$, was computed by the following:

$$\Delta d = (v_o + \Delta v / 2)\, \Delta t\, \underline{\dot{x}} / (\underline{\dot{x}} - v_o - \Delta v / 2) \qquad (2)$$

Missile acceleration, a, was determined from the following (integration being unnecessary):

$$a = \frac{dv}{dt} = q\, \alpha\, (u - v)^2 / u^2 \qquad (3)$$

where q, u, and v are dynamic pressure, wind velocity, and missile velocity at any time t. (Note that an acceleration numeric is used in Chap. 3: $A = a/g$ where g is the acceleration of gravity.)

Equations (1) and (2) were integrated in a stepwise fashion from the arrival time of the blast wave (t = 0) to the time of zero wind velocity (t = $t_u^+$). Because of rapid changes in missile and wind velocities shortly after the arrival of the blast wave, it was necessary to use smaller time steps during the early times than during later times. The following arbitrary scheme was used to determine the variable time step. The first step was always $0.001\, t_u^+$. The remaining time ($t_u^+ - 0.001\, t_u^+$) was divided into 99 log intervals. The first 85 of the log intervals were used as ever-increasing time

-4-

steps. The 85th log interval was then used as a constant time step until time $t_u^+$ was reached.

For convenience, the scaling laws for translational studies derived in Chaps. 2 and 5 of Ref. 1 will be restated using the terminology of the present report. The subscript "1" is used to denote parameters applicable to a yield of 1 ton of high explosives, to an ambient speed of sound of 1117 ft/sec, and to an ambient pressure of 14.7 psi. The parameters without subscripts are applicable to a yield of W tons, to an ambient speed of sound of $c_o$ ft/sec, and to an ambient pressure of $p_o$ psi. Thus, the results in Chap. 3 can be scaled as follows:

$$v = v_1 \, (c_o/1117)$$

$$d = d_1 \, (14.7 \, W/p_o)^{1/3}$$

$$A = A_1 \, (c_o/1117)^2 \, (1/W)^{1/3} \, (p_o/14.7)^{1/3}$$

$$t = t_1 \, (1117/c_o) \, (14.7 \, W/p_o)^{1/3}$$

$$a = a_1 \, (14.7/p_o)^{2/3} \, (c_o/1117)^2 \, (1/W)^{1/3}$$

where

$v$ = missile velocity in ft/sec,

$c_o$ = ambient speed of sound in ft/sec,

$d$ = distance of missile travel in ft,

$W$ = yield of high explosives in tons,

$p_o$ = ambient pressure in psi,

$A$ = acceleration of missile ($A = a/32.2$) in gravity units,

$t$ = time after arrival of blast wave in msec,

$a$ = acceleration coefficient ($a = s \, C_d/m$) in ft$^2$/lb.

## 2.2    BLAST-WAVE PARAMETERS

### 2.2.1    General

The solution of the translation model described in the last section requires that dynamic pressure (q) and wind velocity (u) be

-5-

defined as a function of time. Clear and explicit presentations of these quantities for high explosives were not found in the literature. Consequently, most of the blast material used in this report was taken from a numerical study by Brode[2] and from experimental results reported by Goodman.[3] This material along with Rankine-Hugoniot equations[4] allowed computation of the needed blast parameters. The overpressure-time relation, needed to determine wind velocity as a function of time, will be treated first.

2.2.2    Overpressure vs. Time

The overpressure information was obtained from experimental results.[3] Duration and overpressure impulse scaled to 1 ton of high explosives are recorded in Table 2.1 for the overpressure values of interest in this study. Overpressure as a function of time was not defined in Ref. 3, but in the present report it was assumed to be of the form

$$P = P_s (1 - T)e^{-nT} \tag{4}$$

where

$P$ = overpressure in atm,

$P_s$ = maximum or shock overpressure in atm,

$T = t/t_p^+$,

$t$ = time after arrival of the blast wave in msec,

$t_p^+$ = duration of positive overpressure in msec, and

$n$ = a constant for a given value of $P_s$.

Since n in the above equation determines the shape of the P-t curve, it also determines the impulse, $\int_0^{t_p^+} P\, dt$, for particular values of $P_s$ and $t_p^+$. Thus, integrating Eq. (4) gives the following impulse, $I_p^+$, relation:

$$I_p^+ = P_s t_p^+ (e^{-n} + n - 1)/n^2 \tag{5}$$

The values of n listed in Table 2.1 were found using Eq. (5).

Table 2.1

Parameters for Determining Overpressure-time Functions*
(1 Ton of High Explosives, Surface Burst)

| $P_s$, atm | $t_p^+$, msec | $I_p^+$, atm msec | n |
|---|---|---|---|
| 1.0 | 16.5 | 6.48 | .960 |
| 1.5 | 14.4 | 7.55 | 1.32 |
| 2.0 | 12.9 | 8.30 | 1.47 |
| 2.5 | 11.7 | 8.91 | 1.65 |
| 3.0 | 10.9 | 9.46 | 1.81 |
| 4.0 | 9.70 | 10.3 | 2.15 |
| 5.0 | 8.87 | 10.9 | 2.42 |
| 6.0 | 8.40 | 11.4 | 2.80 |
| 8.0 | 7.99 | 12.2 | 3.63 |
| 10.0 | 7.73 | 12.7 | 4.40 |
| 15.0 | 6.27 | 13.6 | 5.19 |
| 20.0 | 3.00 | 14.2 | 2.65 |

$$*P = P_s (1 - T) e^{-nT} \qquad \text{where } T = t/t_p^+$$

## 2.2.3 Dynamic Pressure vs. Time

Dynamic pressure in atmospheres at the shock front, $Q_s$, was computed using the Rankine-Hugoniot relation reported in Ref. 4:

$$Q_s = \frac{2.5 \, P_s^2}{7 + P_s} \qquad (6)$$

Values of $Q_s$ corresponding to $P_s$ values used in this study are listed in the second column of Table 2.2. Durations, $t_u^+$, and impulses, $I_u^+$, for dynamic pressure in the same table were obtained by scaling the results of a numerical study[2] to a yield of 1 ton (surface burst). A scaling factor was applied to the numerical results in order to make the overpressure durations consistent with those found experimentally.[3]

A procedure similar to that described in Sect. 2.2.2 was used to determine dynamic pressure vs. time. Values recorded in Table 2.2 for r were obtained from

$$I_u^+ = Q_s \, t_u^+ \, (e^{-r} + r - 1)/r^2 \qquad (7)$$

where

$Q_s$ = maximum or shock dynamic pressure in atm,

$t_u^+$ = duration of positive dynamic pressure in msec, and

$r$ = a constant for a particular value of $P_s$ or $Q_s$.

Dynamic pressure as a function of time could then be found using

$$Q = Q_s \, (1 - T) \, e^{-rT}$$

where $T = t/t_u^+$.

## 2.2.4 Wind Velocity vs. Time

By definition,

$$q = 1/2 \, \rho \, u^2 \qquad (8)$$

where   $q$ = dynamic pressure,

Table 2.2

Parameters for Determining Dynamic Pressure
as a Function of Time*
(1 Ton of High Explosives, Surface Burst)

| $P_s$, atm | $Q_s$, atm** | $t_u^+$, msec | $I_u^+$, atm msec | $r$ |
|---|---|---|---|---|
| 1.0 | .3125 | 23.4 | 1.56 | 3.33 |
| 1.5 | .6618 | 20.4 | 2.14 | 5.10 |
| 2.0 | 1.111 | 18.4 | 2.72 | 6.32 |
| 2.5 | 1.645 | 17.1 | 3.26 | 7.47 |
| 3.0 | 2.250 | 16.1 | 3.80 | 8.39 |
| 4.0 | 3.636 | 14.4 | 4.80 | 9.80 |
| 5.0 | 5.208 | 13.1 | 5.77 | 10.7 |
| 6.0 | 6.923 | 11.9 | 6.65 | 11.3 |
| 8.0 | 10.667 | 9.85 | 8.68 | 11.0 |
| 10.0 | 14.706 | 8.17 | 10.81 | 10.0 |
| 15.0 | 25.568 | 5.06 | 16.43 | 6.69 |
| 20.0 | 35.556 | 3.00 | 22.19 | 3.46 |

$$*Q = Q_s (1 - T) e^{-rT} \qquad \text{where } T = t/t_u^+$$

$$**\text{Computed from } Q_s = \frac{2.5 P_s^2}{7 + P_s}$$

$\rho$ = air density, and

u = wind velocity.

Wind velocity could thus be determined after the dynamic pressure and the air density were evaluated. The air density across the shock, $\rho_s$, was found using one of the Rankine-Hugoniot equations:[4]

$$\rho_s = \rho_o (7 + 6 P_s)/(7 + P_s) \tag{9}$$

where $\rho_o$ is the ambient air density.

Changes in air density after the passage of the shock were assumed to be adiabatic. Thus,

$$\rho = \rho_s \left(\frac{P + 1}{P_s + 1}\right)^{1/1.4} \tag{10}$$

where $\rho$ = air density when the overpressure is P atm.

REFERENCES    CHAPTER 2

1.  Bowen, I. G., R. W. Albright, E. R. Fletcher and C. S.
    White, A Model Designed to Predict the Motion of Objects
    Translated by Classical Blast Waves, Civil Effects Test Oper-
    ations, USAEC Report CEX-58.9, June 29, 1961.

2.  Brode, Harold L., A Calculation of the Blast Wave From a
    Spherical Charge of TNT, RM-1965, ASTIA Document Number
    AD 144302, August 21, 1957.

3.  Goodman, H. J., Compiled Free-Air Blast Data on Bare
    Spherical Pentolite, BRL Report No. 1092, February 1960.

4.  Glasstone, Samuel, Editor, The Effects of Nuclear Weapons,
    Revised Edition 1962, Superintendent of Documents, U. S.
    Printing Office, Washington, D. C., April 1962.

# CHAPTER 3 RESULTS

## 3.1 GENERAL

Computed results were obtained using the translation model described in Sect. 2.1 and a digital computer with an incremental plotter to graph the output data. The system for determining time steps (see Sect. 2.1) resulted in 106 to 112 steps for each numerical integration from the arrival of the blast wave (t = 0) to the time of zero wind (t = $t_{\overline{w}}^{+}$).

As previously noted, all solutions were made for 1 ton of high explosives burst at the surface. The 12 different blast waves used are identified in terms of overpressure: $P_s = p_s/p_o$, the ratio of shock overpressure to local ambient pressure (not necessarily the sea-level value of 14.7 psi), sometimes called excess pressure ratio. Values of $P_s$ used were 1.0, 1.5, 2.0, 2.5, 3.0, 4.0, 5.0, 6.0, 8.0, 10.0, 15.0, and 20.0 atm.

For each $P_s$, numerical integrations were made for the following acceleration coefficients, $\alpha_1$, in the order listed: 6, 3, 2, 1, 0.6, 0.3, 0.2, 0.1, 0.06, 0.03, 0.02, 0.01 ft$^2$/lb. If the maximum velocity computed for any acceleration coefficient was less than 10 ft/sec, the computations were halted for that overpressure.

According to the translational model used, the behavior of an object is determined by its acceleration coefficient, all other factors being constant. To aid interpretation of the computed results, a list of acceleration coefficients obtained from Ref. 1 for a variety of objects is reproduced in Table 3.1. A more complete source of acceleration-coefficient information can be found in Ref. 2.

## 3.2 VELOCITY VS. TIME AND DISTANCE VS. TIME

Computed velocity and distance as functions of time are presented for a maximum overpressure* of 1 atm in Figs. 3.1 and 3.2, respectively, for seven acceleration coefficients. Machine plots for these and succeeding figures connected with straight lines every other computed point for the first 86 time steps. All of the remaining time steps were plotted. Each of the curves end at the midpoint of the last time step before the dynamic pressure

---

*Defined in Sect. 3.1.

Table 3.1

Typical Acceleration Coefficients,* $a = sC_d/m$
where s is the area presented to wind by missile,
$C_d$ is the drag coefficient of the missile,
and m is the mass of the missile

| | $a$, ft$^2$/lb |
|---|---|
| 168-lb man: | |
|     Standing facing wind | 0.052 |
|     Standing sidewise to wind | 0.022 |
|     Couching facing wind | 0.021 |
|     Couching sidewise to wind | 0.017 |
|     Prone aligned with wind | 0.0063 |
|     Prone perpendicular to wind | 0.022 |
|     Average value for tumbling man in straight, rigid position | 0.03 |
| 21-g mice, maximum area presented to wind | 0.38 |
| 180-g rats, maximum area presented to wind | 0.19 |
| 530-g guinea pigs, maximum area presented to wind | 0.15 |
| 2100-g rabbits, maximum area presented to wind | 0.079 |
| Typical stones: | |
|     0.1 g | 0.67 |
|     1.0 g | 0.32 |
|     10.0 g | 0.15 |
| Window-glass fragments, 1/8 in. thick** | |
|     0.1 g, all orientations | 0.78 |
|     1.0 g, edgewise and broadside to wind | 0.48-0.57 |
|     10.0 g, edgewise and broadside to wind | 0.34-0.72 |

*From Ref. 1.
**Single-strength window glass. See Ref. 2 for data on plate glass.

Computed for: $P_s = 1.0$ atm; $W = 1$ ton; $p_o = 14.7$ psi; and $c_o = 1117$ ft/sec

For other conditions use: $\alpha_1 = \alpha (1117/c_o)^2 (p_o/14.7)^{2/3} W^{1/3}$, $t = t_1 (1117/c_o)(14.7 W/p_o)^{1/3}$;

and $v = v_1 (c_o/1117)$

$\alpha_1 = 6$

Velocity, $v_1$, ft/sec

Time, $t_1$, msec
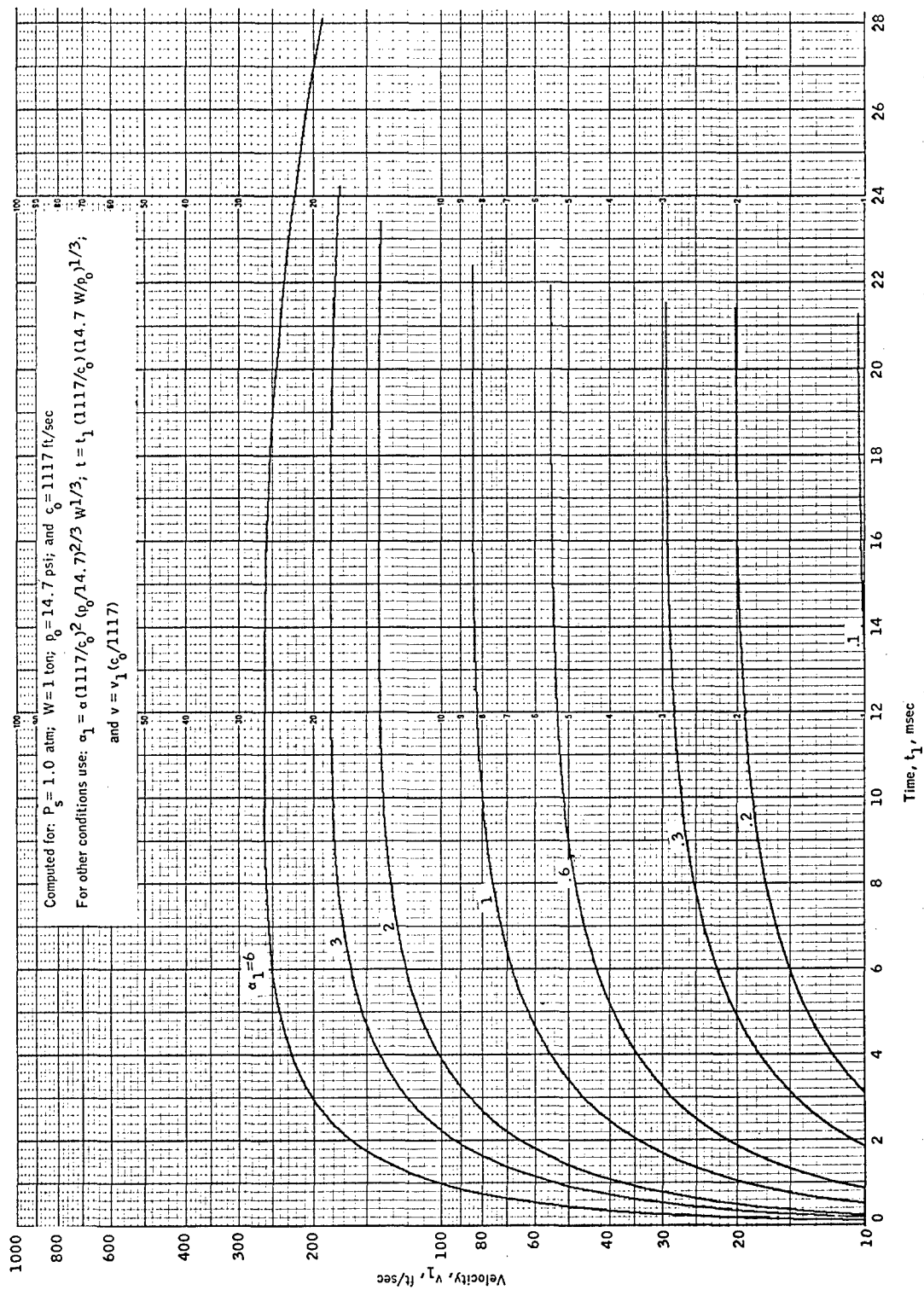
Fig. 3.1   Velocity vs. Time for $P_s = 1.0$ atm

Computed for: $P_s = 1.0$ atm; $W = 1$ ton; $p_o = 14.7$ psi; and $c_o = 1117$ ft/sec

For other conditions use: $c_1 = c (1117/c_o)^2 (p_o/14.7)^{2/3} W^{1/3};$   $t = t_1 (1117/c_o)(14.7 W/p_o)^{1/3};$

and $d = d_1 (14.7 W/p_o)^{1/3}$

Time, $t_1$, msec
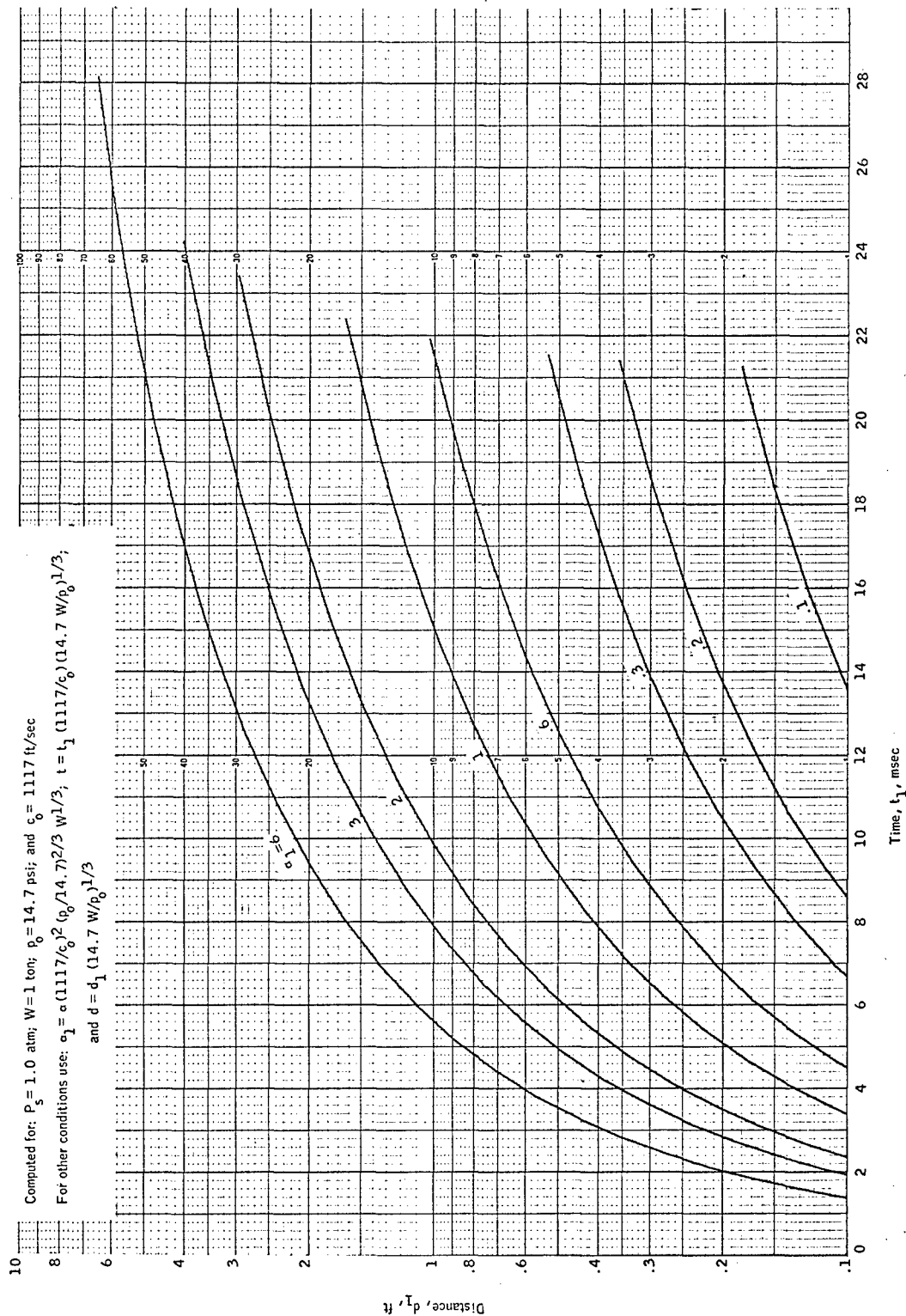
Distance, $d_1$, ft

Fig. 3.2   Distance vs. Time for $P_s = 1.0$ atm

15

and winds become negative. For high acceleration coefficients, the curves terminate at later times than do those for low ones: the missiles with high coefficients — and, thus, with high veloc- ities — travel along with the blast wave for longer times than do those with the low ones.

The appropriate equations for scaling the computed results to other yields and ambient pressures and speeds of sound are presented on each chart. To illustrate scaling from 1 ton to 1000 tons (1 kt) and to compare the results for 1 kt with those for nuclear blast waves,[1] consider the maximum velocity and distance of travel at maximum velocity predicted for a 1-gm stone when $p = 1.0$ atm, $p_o = 14.7$ psi, $c_o = 1117$ ft/sec. A stone of 1 gm has an acceleration coefficient of $0.32$ ft$^2$/lb. (See Table 3.1.) For a yield of 1 ton the maximum predicted velocity for $a_1 = 0.32$ ft$^2$/lb obtained from Fig. 3.1 is about 30 ft/sec occurring 19 msec after the arrival of the blast wave. By referring to Fig. 3.2, the distance of travel of 19 msec is found to be about 0.48 ft.

To apply the computed data to a yield of 1000 tons, it is first necessary to determine an equivalent acceleration coefficient, $a_1$, for a yield of 1 ton. By using the scaling equation for accel- eration coefficient in Figs. 3.1 and 3.2, $a_1 = 0.32$ ft$^2$/lb x $(1000)^{1/3}$ $= 3.2$ ft$^2$/lb. The maximum velocity predicted for this value of $a_1$ is about 185 ft/sec occurring 15 msec after the arrival of the blast wave (Fig. 3.1). The distance traveled for $W = 1$ ton and for $a_1 = 3.2$ ft$^2$/lb at 15 msec is 2.4 ft (Fig. 3.2). For $W = 1000$ tons, the distance is 2.4 ft x $(1000)^{1/3} = 24$ ft occurring 15 msec x $(1000)^{1/3} = 150$ msec after the arrival of the blast wave. For com- parison, the maximum velocity and distance of travel at maximum velocity computed for a nuclear blast wave[1] for the conditions stated above for a yield of 1 kt are 200 ft/sec (high explosives: 185 ft/sec) and 28.7 ft (high explosives: 24 ft). Similar comparisons for lower acceleration coefficients, however, showed a larger discrepancy between the velocities and distances predicted for the high-explosive and nuclear blast waves. The explanation of this is that the blast criteria used for $P_s = 1$ atm indicates a shorter duration of dynamic pressure for the high-explosive than for the nuclear blast wave for the same explosive yield, maximum overpressure, and ambient pressure and speed of sound. Duration effects on maximum velocity are less pronounced for the high acceleration coefficients than for the low ones since the former reach maximum velocity before the blast wave has decayed appreciably.

The charts shown in Figs. 3.3 to 3.24, similar to those described, were computed for maximum overpressures of 1.5, 2.0, 2.5, 3.0,

Computed for: $P_s = 1.5$ atm; $W = 1$ ton; $p_0 = 14.7$ psi; and $c_0 = 1117$ ft/sec

For other conditions use: $a_1 = a (1117/c_0)^2 (p_0/14.7)^{2/3} W^{1/3}$; $t = t_1 (1117/c_0) (14.7 \ W/p_0)^{1/3}$;

and $v = v_1 (c_0/1117)$

Velocity, $v_1$, ft/sec

Time, $t_1$, msec
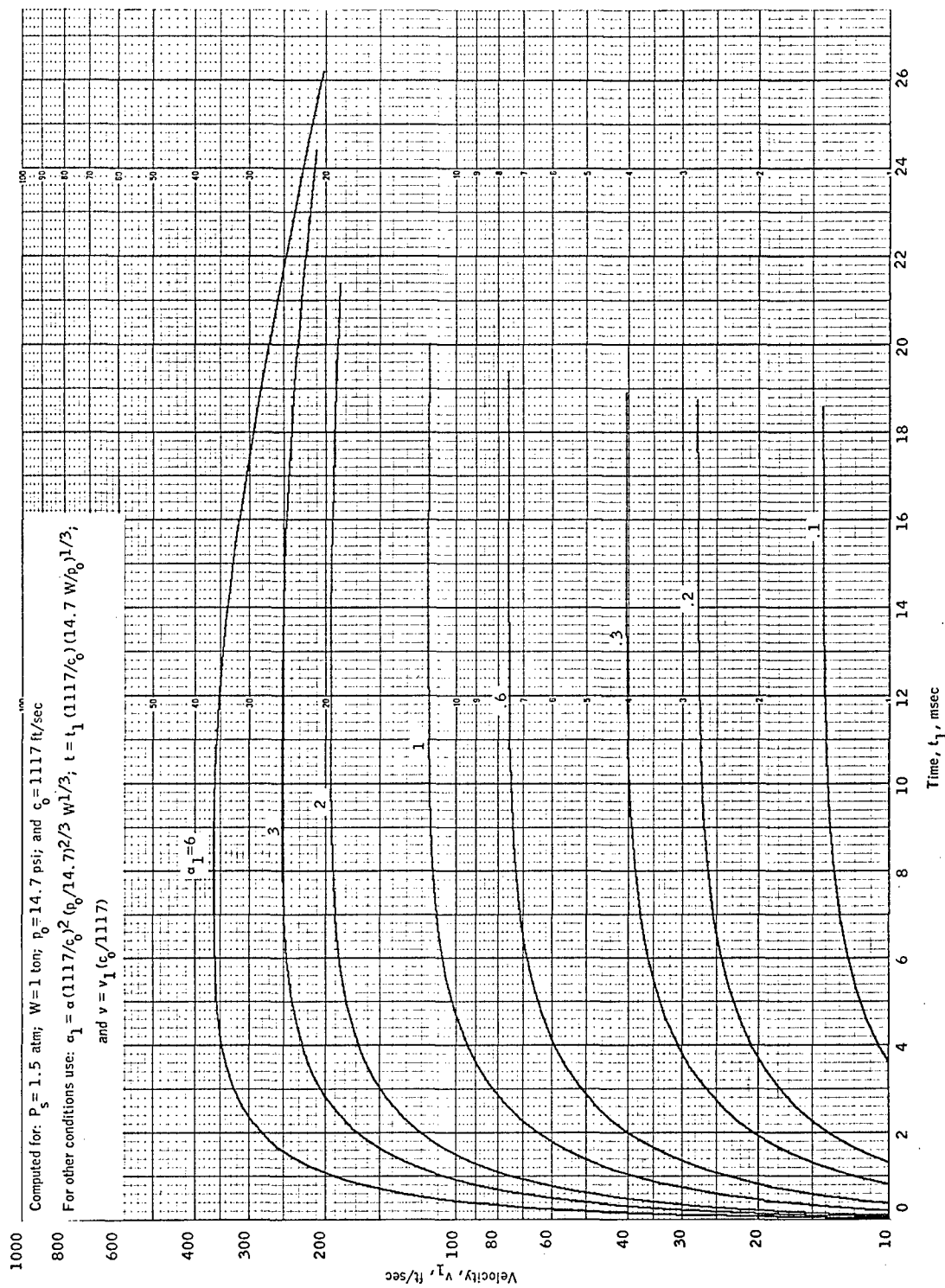
Fig. 3.3   Velocity vs. Time for $P_s = 1.5$ atm

17

Computed for: $P_s = 1.5$ atm; $W = 1$ ton; $p_o = 14.7$ psi; and $c_o = 1117$ ft/sec

For other conditions use: $a_1 = a(1117/c_o)^2 (p_o/14.7)^{2/3} W^{1/3}$; $t = t_1 (1117/c_o)(14.7 W/p_o)^{1/3}$;

and $d = d_1 (14.7 W/p_o)^{1/3}$

Distance, $d_1$, ft

Time, $t_1$, msec
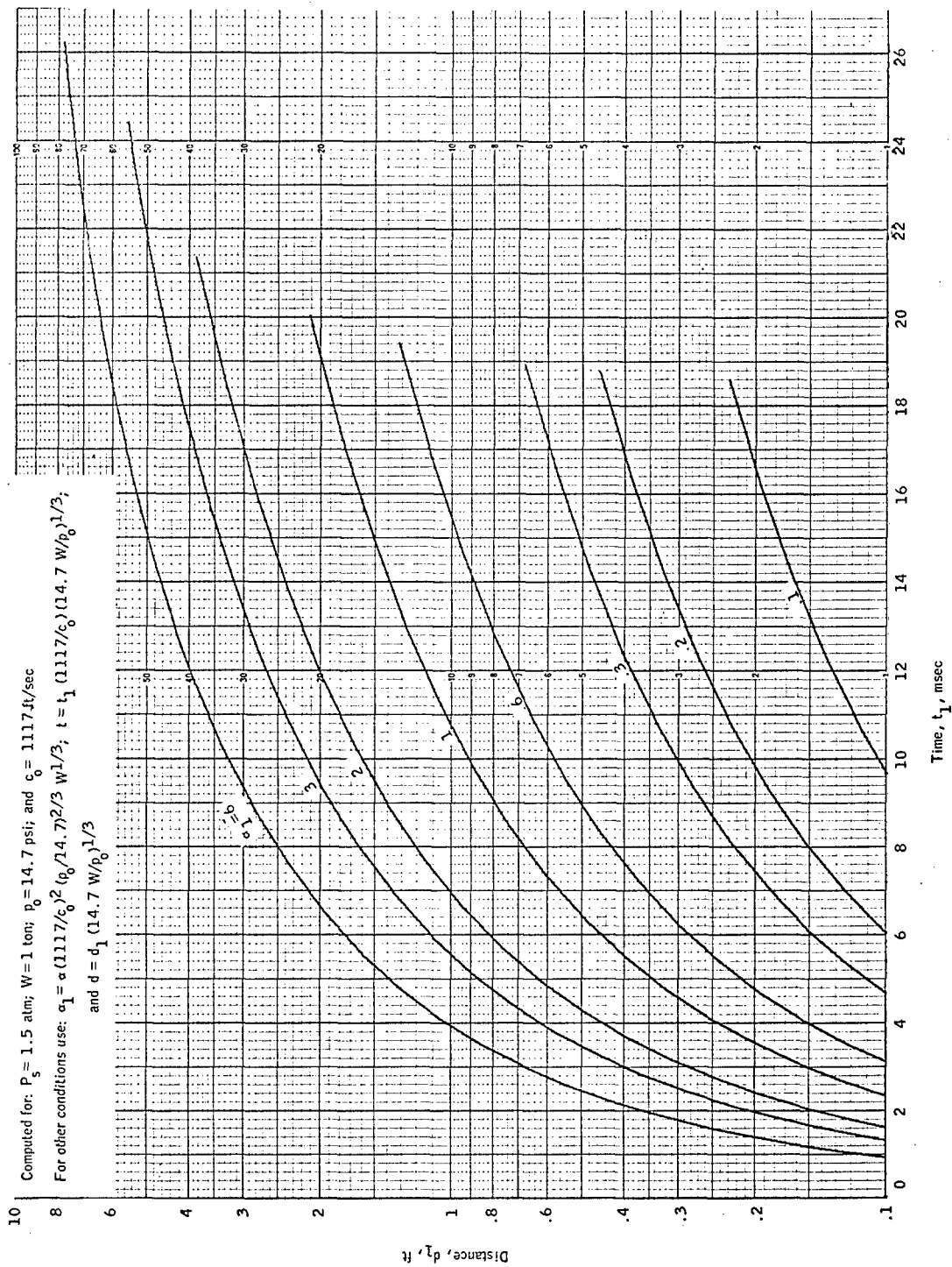
Fig. 3.4   Distance vs. Time for $P_s = 1.5$ atm

18

Computed for: $P_s = 2.0$ atm; $W = 1$ ton; $p_o = 14.7$ psi; and $c_o = 1117$ ft/sec

For other conditions use: $a_1 = a(1117/c_o)^2 (p_o/14.7)^{2/3} W^{1/3}$; $t = t_1 (1117/c_o)(14.7 W/p_o)^{1/3}$;

and $v = v_1 (c_o/1117)$
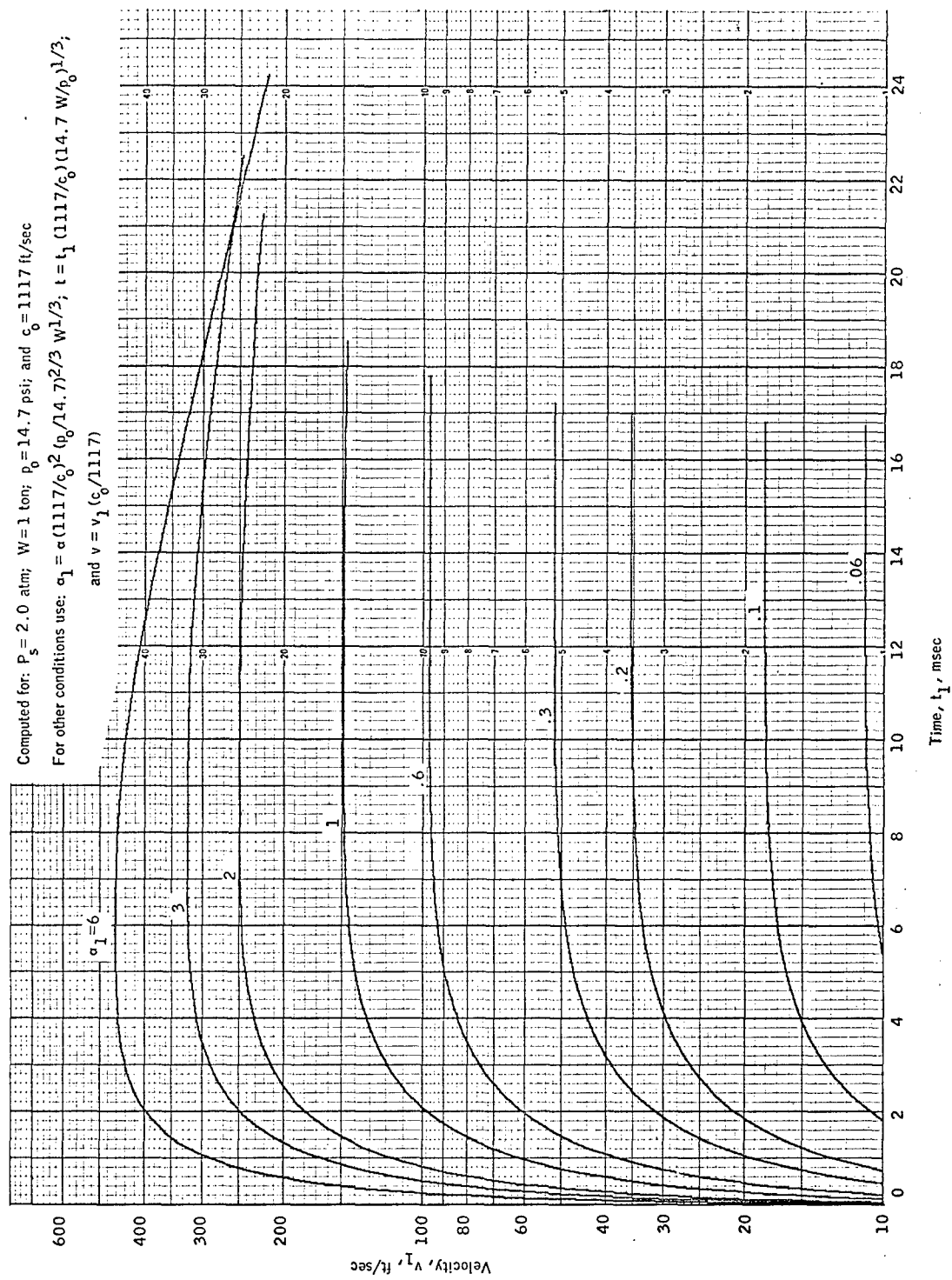
Fig. 3.5   Velocity vs. Time for $P_s = 2.0$ atm

19

Fig. 3.6   Distance vs. Time for $P_s$ = 2.0 atm

Computed for:  $P_s$ = 2.0 atm;  W = 1 ton;  $p_o$ = 14.7 psi;  and  $c_o$ = 1117 ft/sec

For other conditions use:  $a_1 = a \, (1117/c_o)^2 \, (p_o/14.7)^{2/3} \, W^{1/3}$,   $t = t_1 \, (1117/c_o) \, (14.7 \, W/p_o)^{1/3}$;

and  $d = d_1 \, (14.7 \, W/p_o)^{1/3}$

Time, $t_1$, msec

Distance, $d_1$, ft

20

Computed for: $P_s = 2.5$ atm; $W = 1$ ton; $p_0 = 14.7$ psi; and $c_0 = 1117$ ft/sec

For other conditions use: $\alpha_1 = \alpha (1117/c_0)^2 (p_0/14.7)^{2/3} W^{1/3}$; $t = t_1 (1117/c_0)(14.7 W/p_0)^{1/3}$;

and $v = v_1 (c_0/1117)$
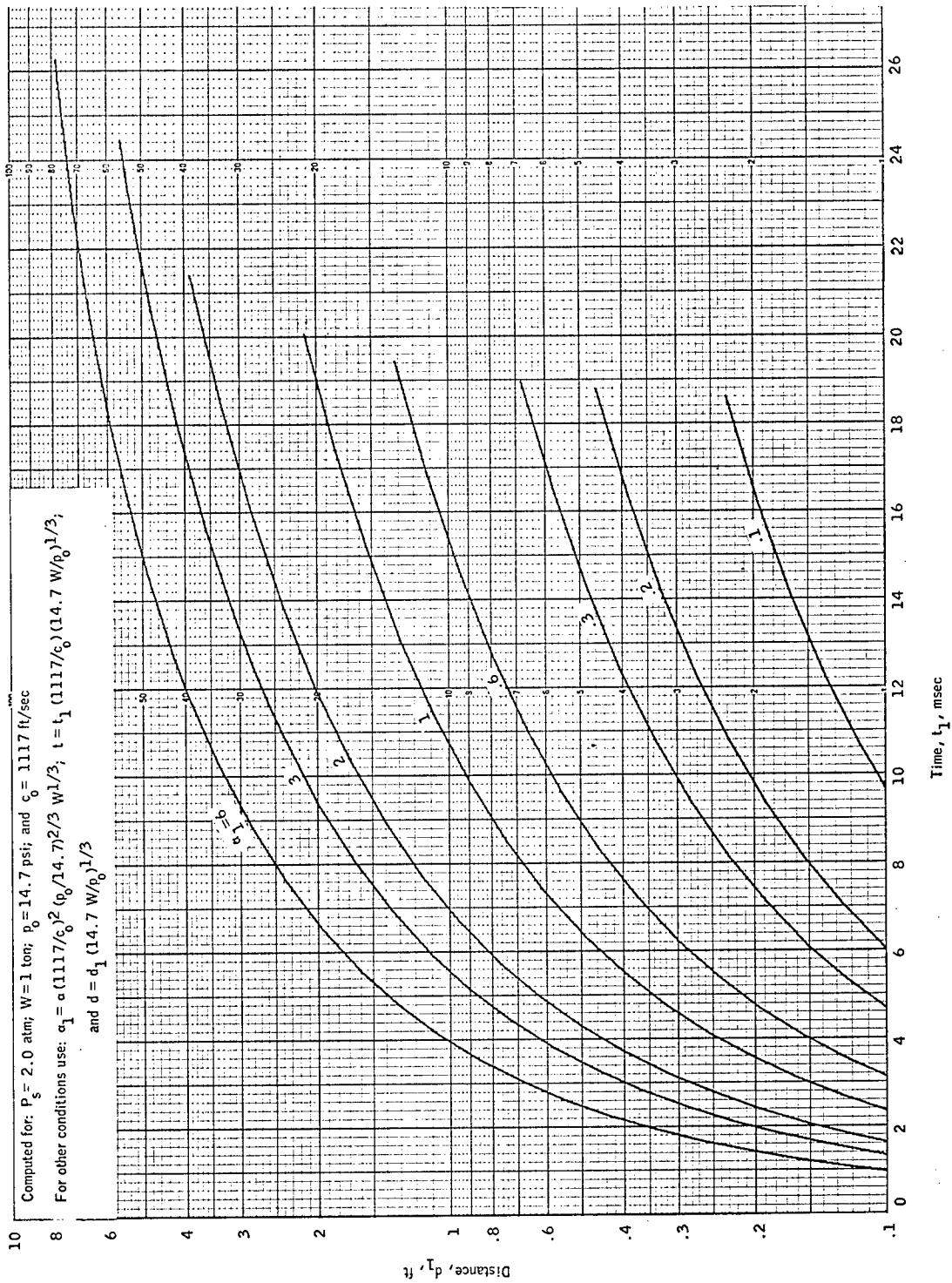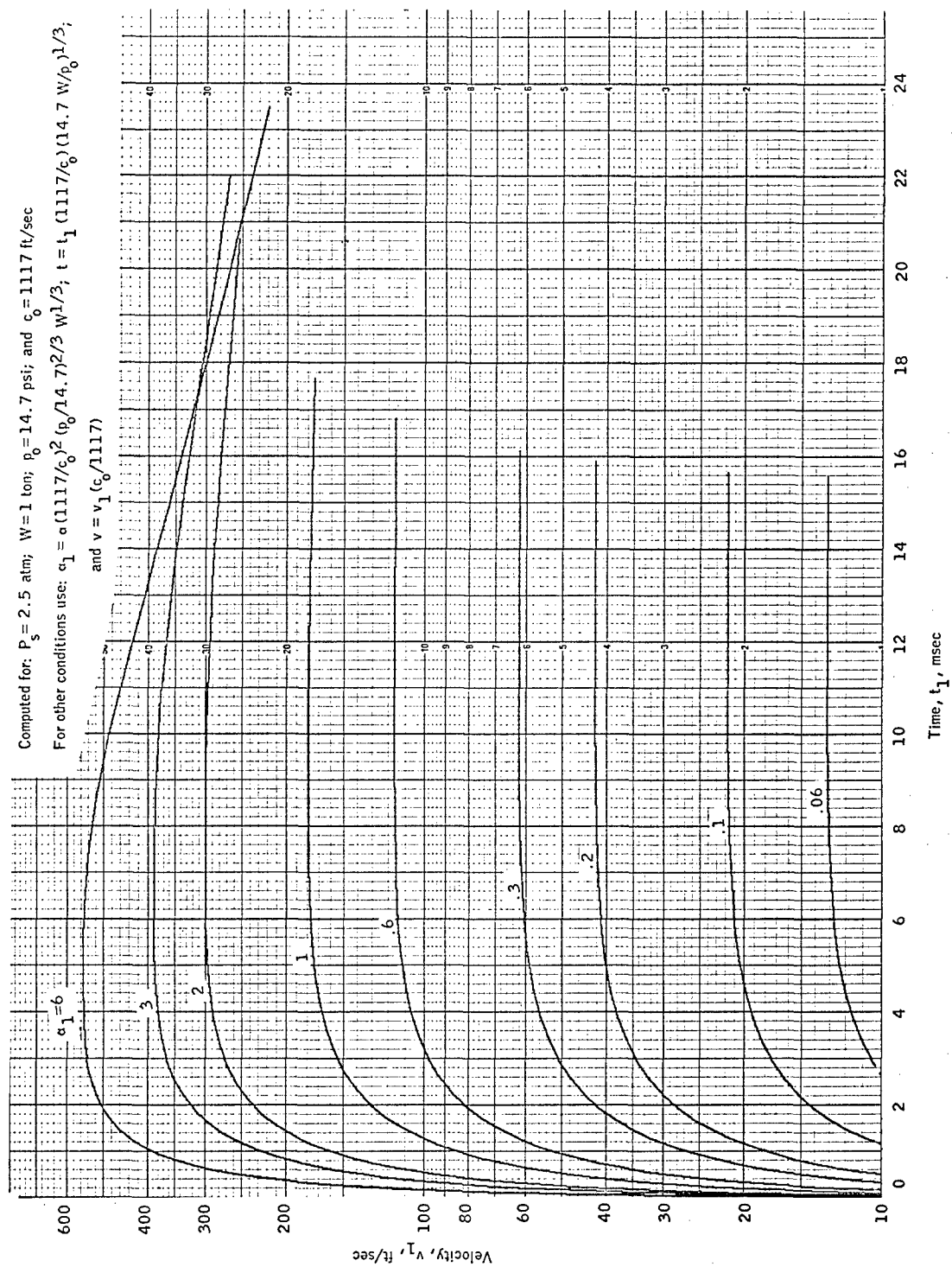
Fig. 3.7   Velocity vs. Time for $P_s = 2.5$ atm

21

Computed for: $P_s = 2.5$ atm; $W = 1$ ton; $p_o = 14.7$ psi; and $c_o = 1117$ ft/sec

For other conditions use: $a_1 = a(1117/c_o)^2 (p_o/14.7)^{2/3} W^{1/3}$, $t = t_1 (1117/c_o)(14.7 W/p_o)^{1/3}$;

and $d = d_1 (14.7 W/p_o)^{1/3}$

Time, $t_1$, msec

Distance, $d_1$, ft
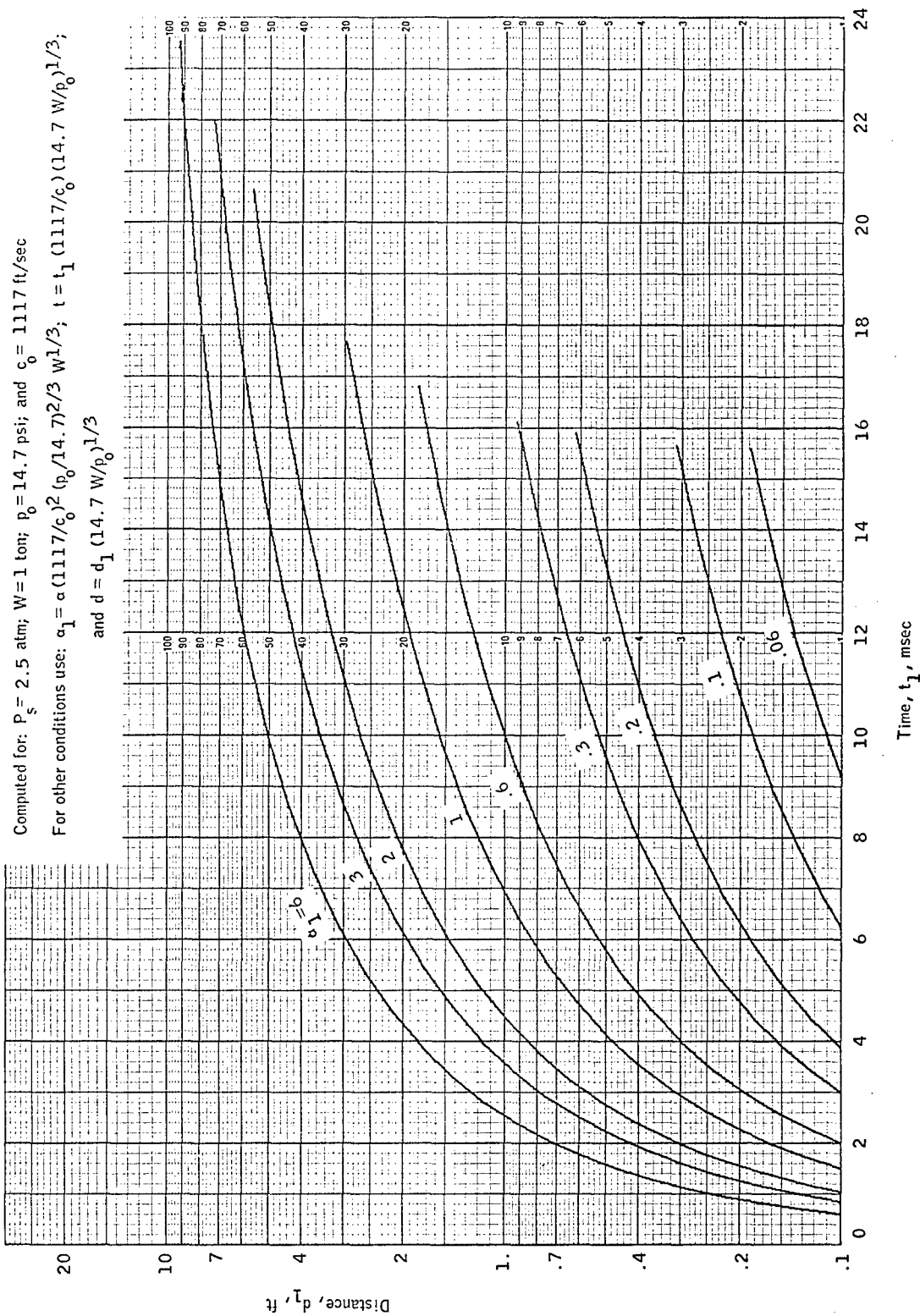
Fig. 3.8   Distance vs. Time for $P_s = 2.5$ atm

22

Computed for: $P_s = 3.0$ atm; $W = 1$ ton; $p_o = 14.7$ psi; and $c_o = 1117$ ft/sec

For other conditions use: $\alpha_1 = \alpha(1117/c_o)^2(p_o/14.7)^{2/3} W^{1/3}$; $t = t_1(1117/c_o)(14.7\ W/p_o)^{1/3}$;

and $v = v_1(c_o/1117)$
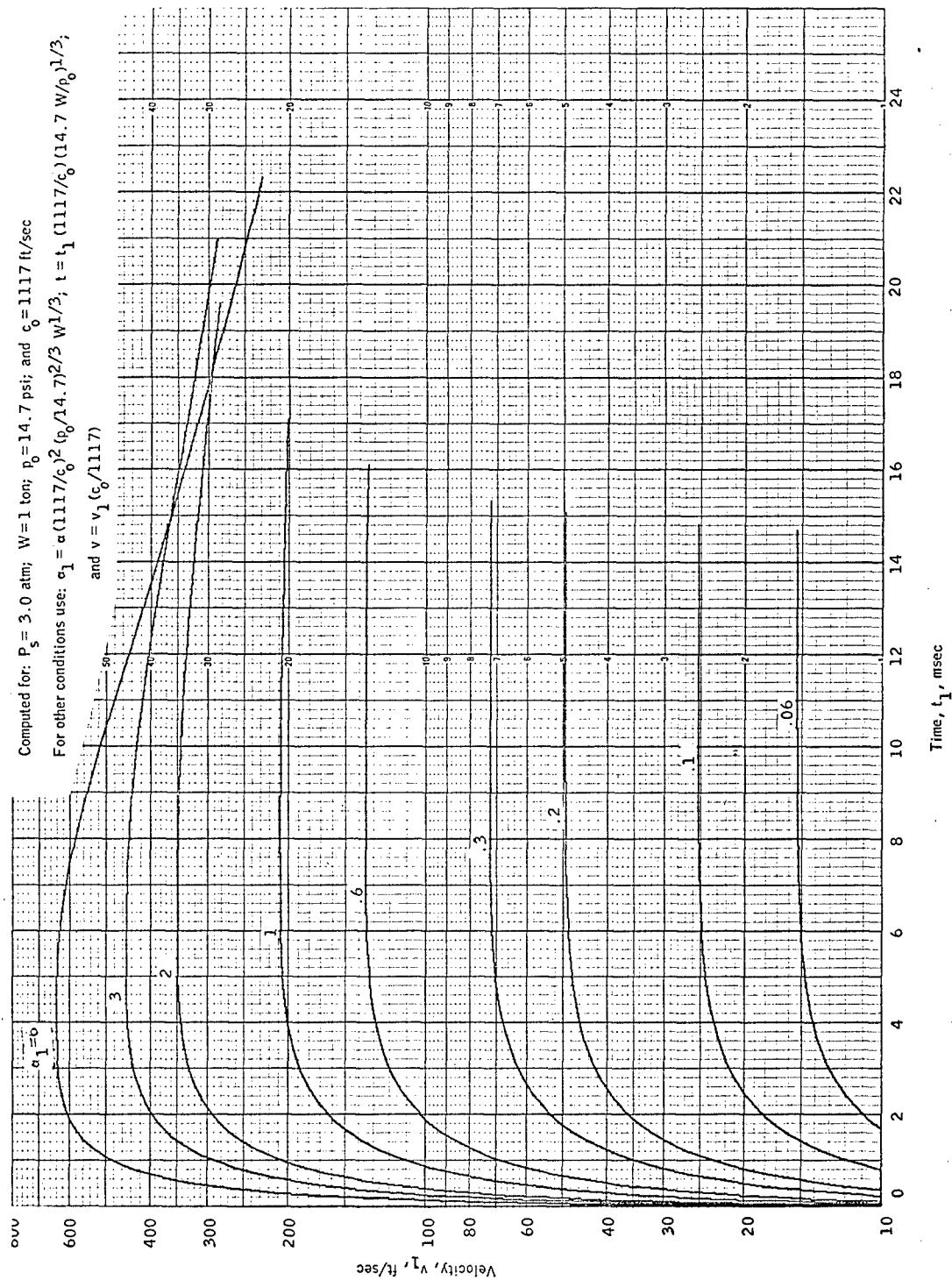
Fig. 3.9   Velocity vs. Time for $P_s = 3.0$ atm

Computed for: $P_s = 3.0$ atm; $W = 1$ ton; and $p_0 = 14.7$ psi; and $c_0 = 1117$ ft/sec

For other conditions use: $\alpha_1 = \alpha (1117/c_0)^2 (p_0/14.7)^{2/3} W^{1/3}$; $t = t_1 (1117/c_0)(14.7 W/p_0)^{1/3}$;

and $d = d_1 (14.7 W/p_0)^{1/3}$

Time, $t_1$, msec

Distance, $d_1$, ft
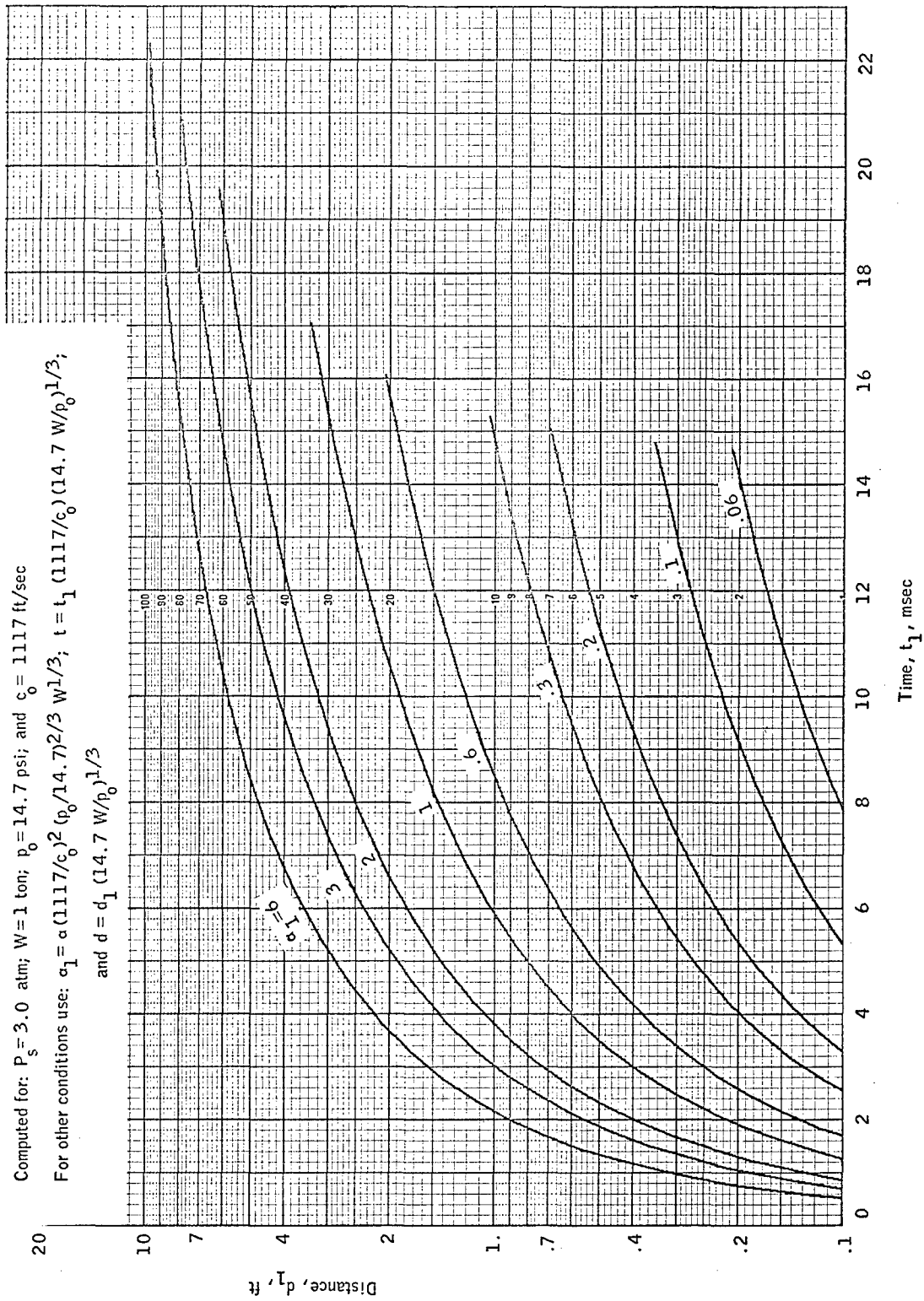
Fig. 3.10 Distance vs. Time for $P_s = 3.0$ atm

24

Computed for: $P_s = 4.0$ atm; $W = 1$ ton; $p_0 = 14.7$ psi; and $c_0 = 1117$ ft/sec

For other conditions use: $a_1 = a (1117/c_0)^2 (p_0/14.7)^{2/3} W^{1/3}$; $t = t_1 (1117/c_0)(14.7 W/p_0)^{1/3}$;

and $v = v_1 (c_0/1117)$
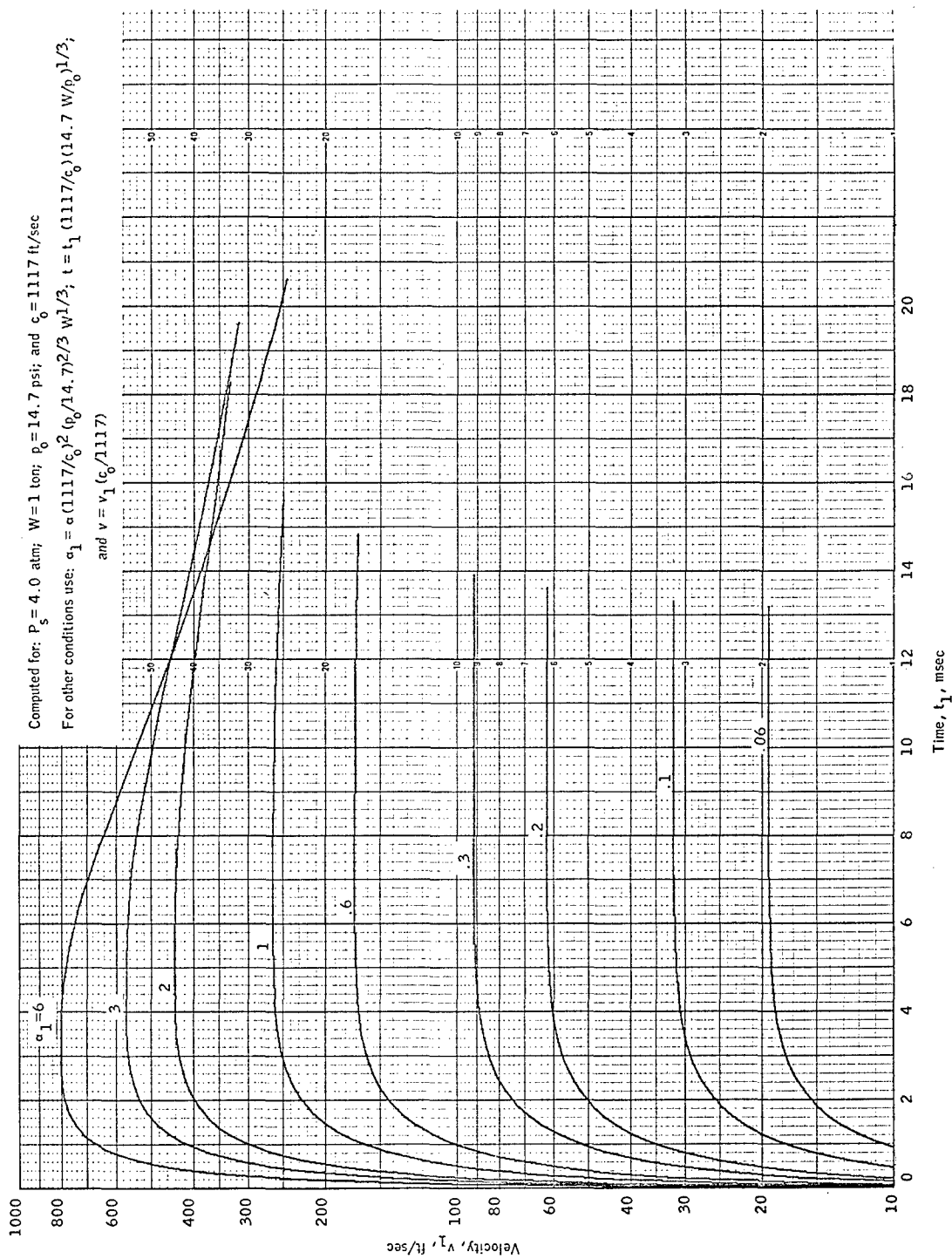
Fig. 3.11   Velocity vs. Time for $P_s = 4.0$ atm

25

Computed for: $P_s = 4.0$ atm; $W = 1$ ton; $p_o = 14.7$ psi; and $c_o = 1117$ ft/sec

For other conditions use: $a_1 = a (1117/c_o)^2 (p_o/14.7)^{2/3} W^{1/3}$; $t = t_1 (1117/c_o) (14.7 \ W/p_o)^{1/3}$;

and $d = d_1 (14.7 \ W/p_o)^{1/3}$
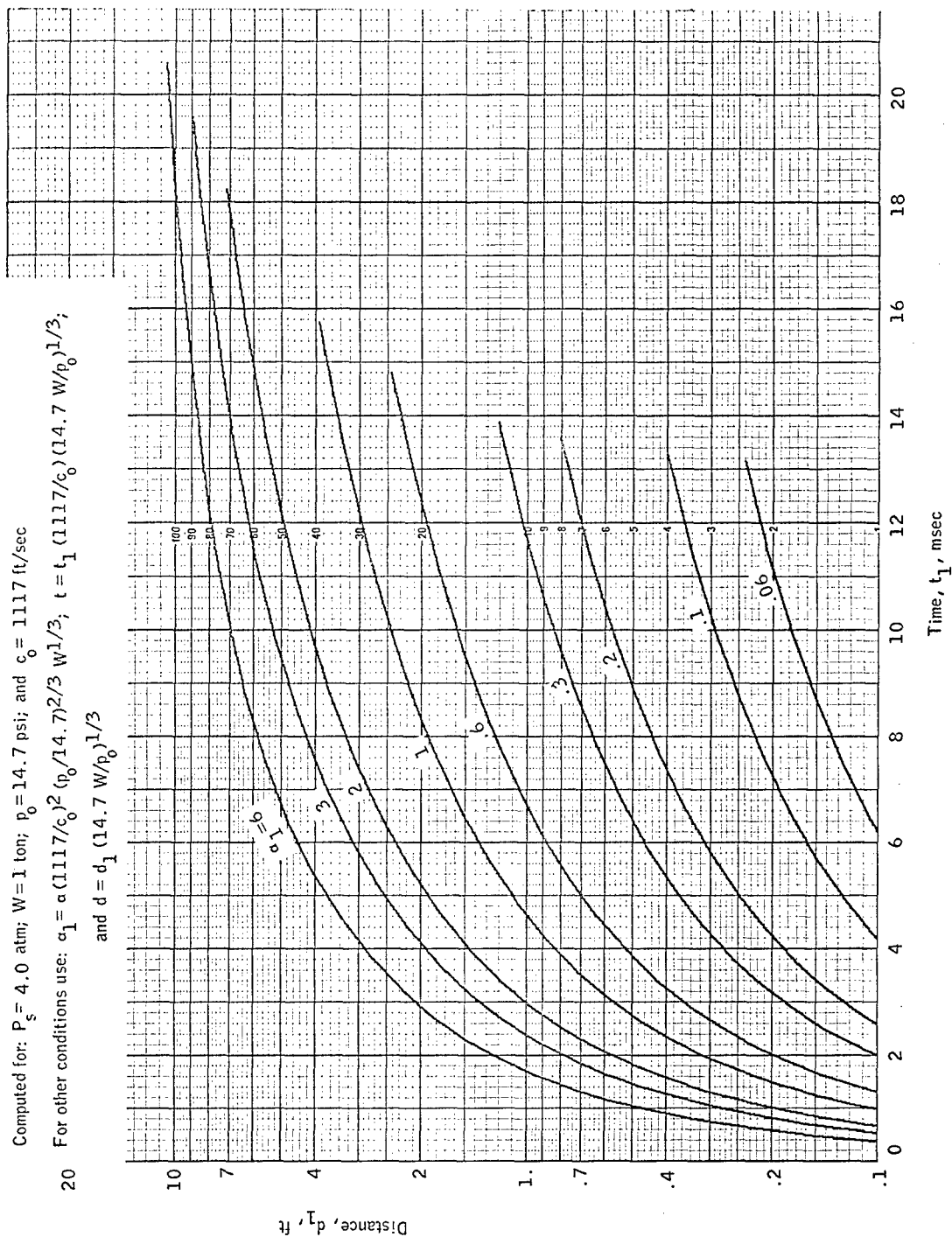
Fig. 3.12  Distance vs. Time for $P_s = 4.0$ atm

26

Fig. 3.13  Velocity vs. Time for $P_s$ = 5.0 atm

Computed for: $P_s$ = 5.0 atm; W = 1 ton; $p_0$ = 14.7 psi; and $c_0$ = 1117 ft/sec

For other conditions use: $a_1 = a (1117/c_0)^2 (p_0/14.7)^{2/3} W^{1/3}$; $t = t_1 (1117/c_0)(14.7 W/p_0)^{1/3}$;

and $v = v_1 (c_0/1117)$

27

Computed for: $P_s = 5.0$ atm; $W = 1$ ton; $p_o = 14.7$ psi; and $c_o = 1117$ ft/sec

For other conditions use: $a_1 = a (1117/c_o)^2 (p_o/14.7)^{2/3} W^{1/3}$; $t = t_1 (1117/c_o)(14.7 \, W/p_o)^{1/3}$;

and $d = d_1 (14.7 \, W/p_o)^{1/3}$
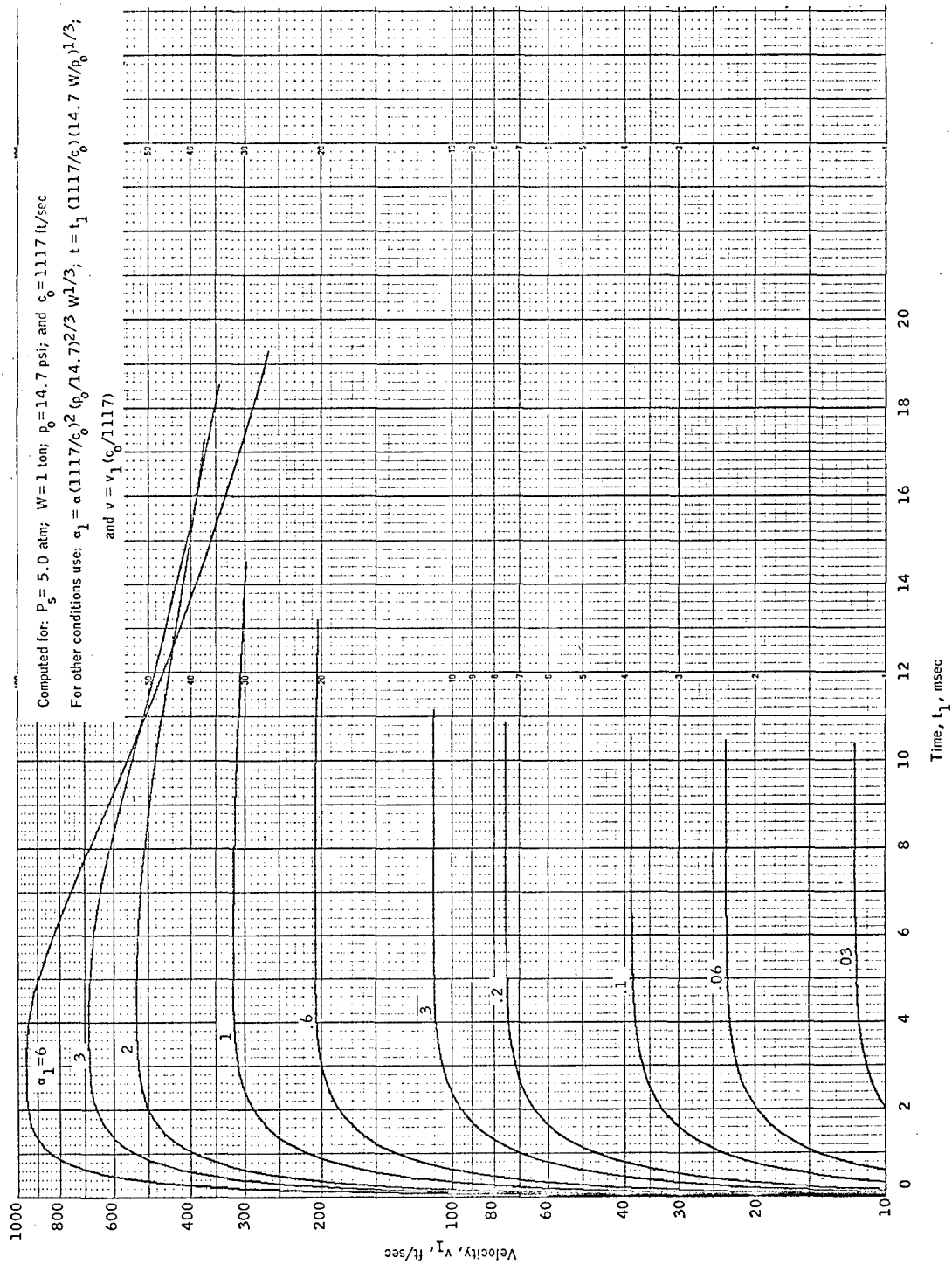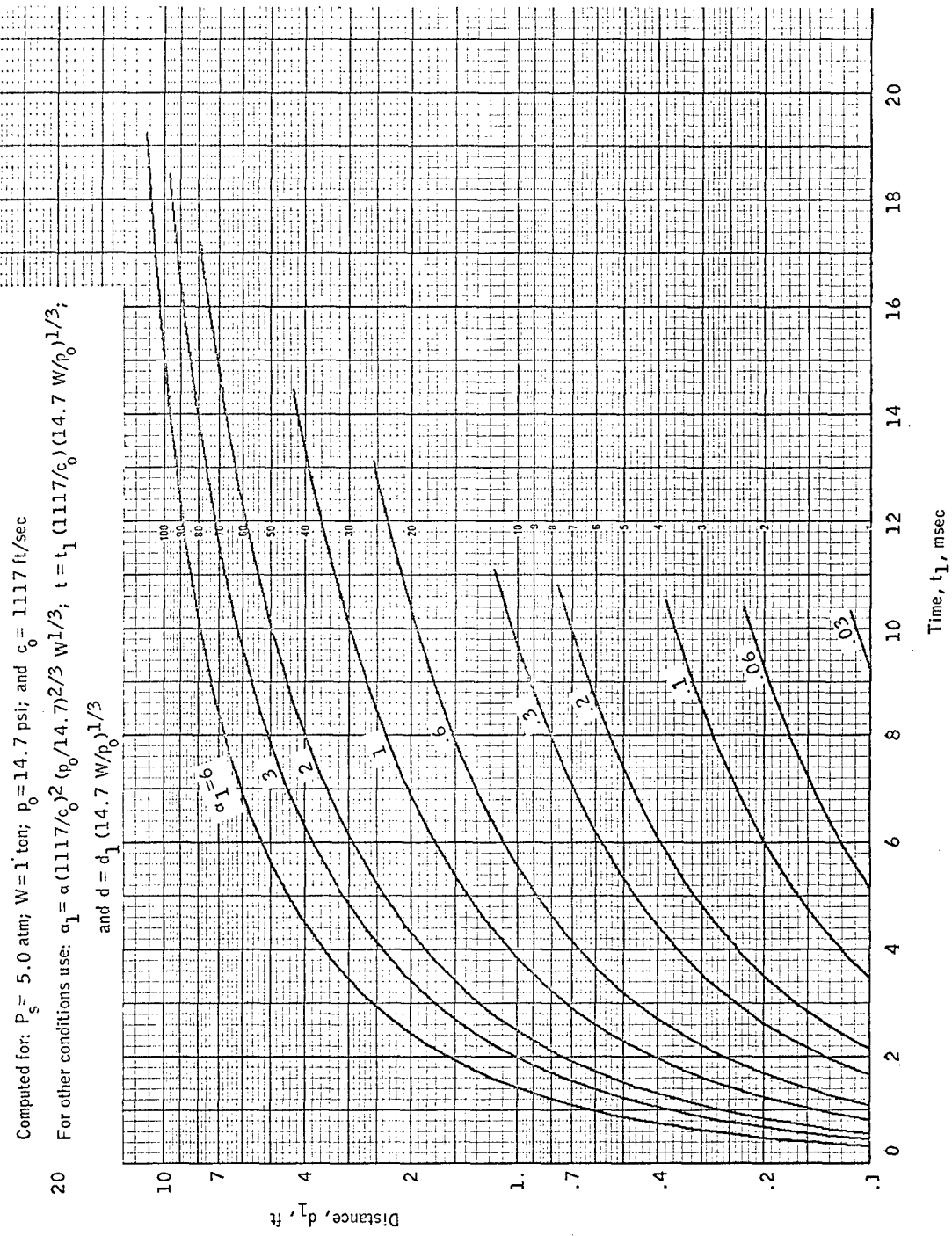


Fig. 3.14   Distance vs. Time for $P_s = 5.0$ atm

Computed for: $P_s = 6.0$ atm; $W = 1$ ton; $p_o = 14.7$ psi; and $c_o = 1117$ ft/sec

For other conditions use: $a_1 = a (1117/c_o)^2 (p_o/14.7)^{2/3} W^{1/3}$; $t = t_1 (1117/c_o)(14.7 \ W/p_o)^{1/3}$;

and $v = v_1 (c_o/1117)$

Fig. 3.15   Velocity vs. Time for $P_s = 6.0$ atm

29

Computed for: $P_s = 6.0$ atm; $W = 1$ ton; $p_o = 14.7$ psi; and $c_o = 1117$ ft/sec

For other conditions use: $a_1 = a(1117/c_o)^2 (p_o/14.7)^{2/3} W^{1/3}$, $t = t_1 (1117/c_o)(14.7 \, W/p_o)^{1/3}$;

and $d = d_1 (14.7 \, W/p_o)^{1/3}$

Fig. 3.16   Distance vs. Time for $P_s = 6.0$ atm

Computed for: $P_s = 8.0$ atm; $W = 1$ ton; $p_o = 14.7$ psi; and $c_o = 1117$ ft/sec

For other conditions use: $a_1 = a (1117/c_o)^2 (p_o/14.7)^{2/3} W^{1/3}$; $t = t_1 (1117/c_o)(14.7 \ W/p_o)^{1/3}$;

and $v = v_1' (c_o/1117)$
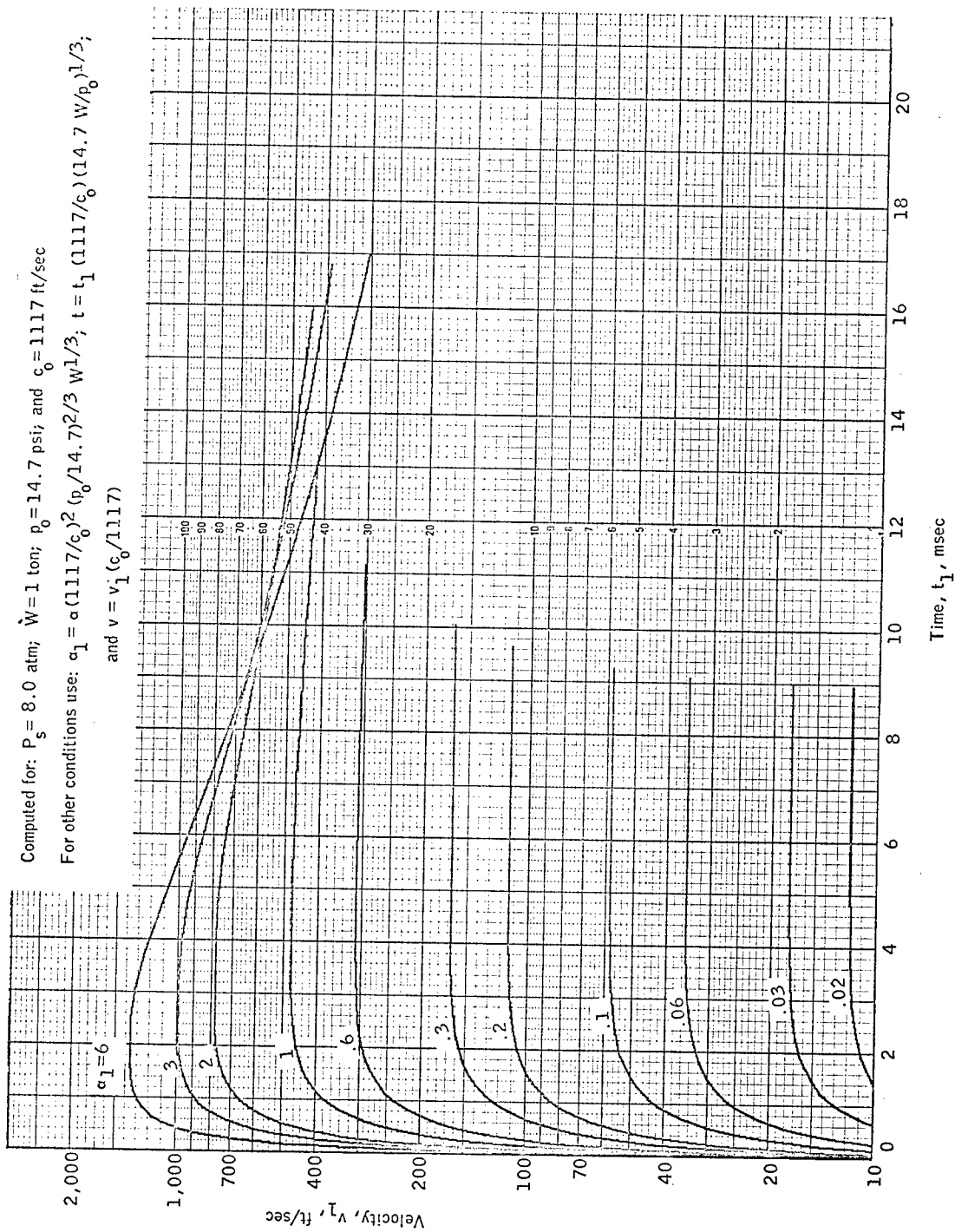
Fig. 3.17   Velocity vs. Time for $P_s = 8.0$ atm

31

Computed for: $P_s = 8.0$ atm; $W = 1$ ton; $p_o = 14.7$ psi; and $c_o = 1117$ ft/sec

For other conditions use: $a_1 = q (1117/c_o)^2 (p_o/14.7)^{2/3} W^{1/3}$; $t = t_1 (1117/c_o)(14.7 \, W/p_o)^{1/3}$;

and $d = d_1 (14.7 \, W/p_o)^{1/3}$
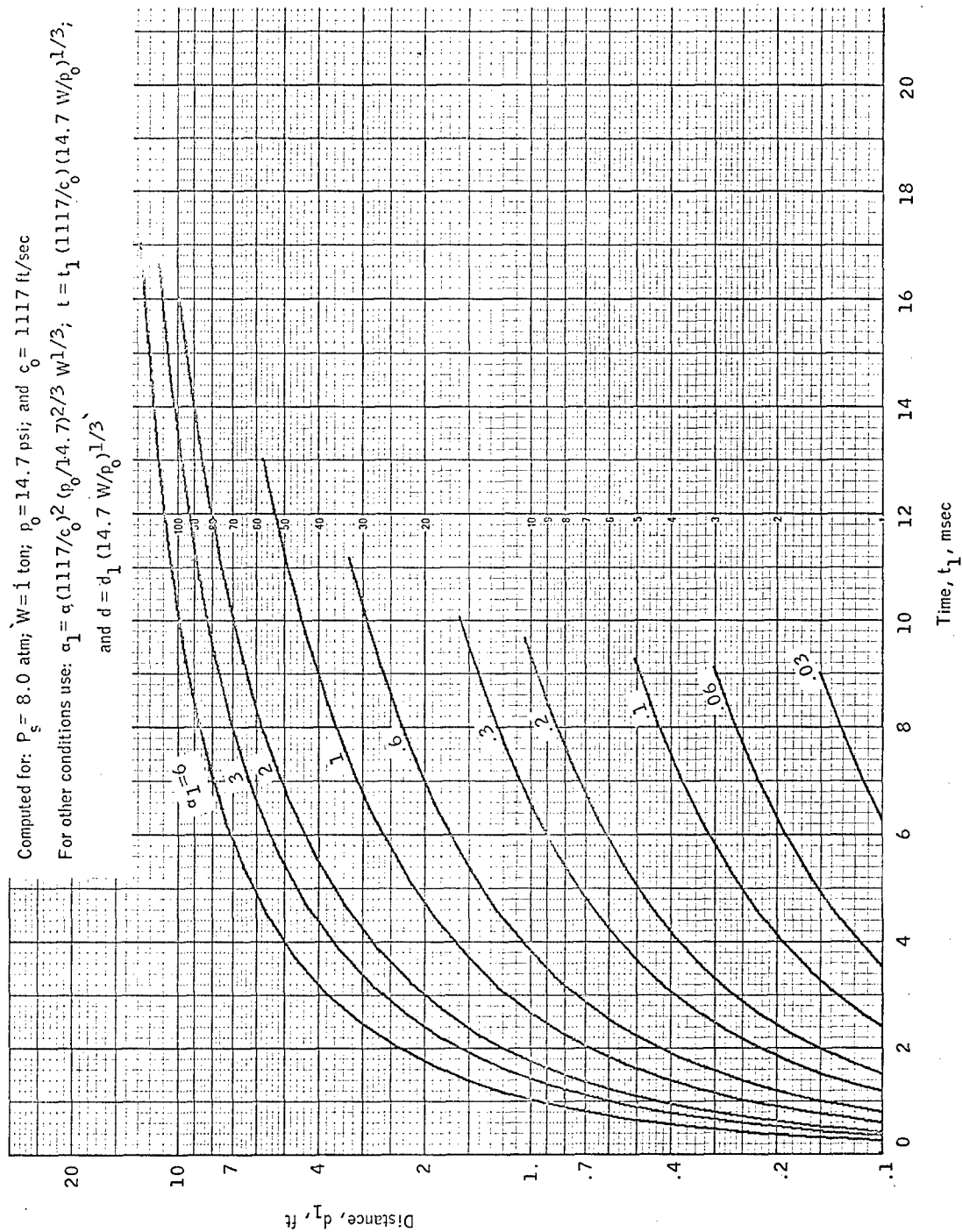
Fig. 3.18   Distance vs. Time for $P_s = 8.0$ atm

32

Computed for: $P_s = 10$ atm; $W = 1$ ton; $p_0 = 14.7$ psi; and $c_0 = 1117$ ft/sec

For other conditions use: $\alpha_1 = \alpha (1117/c_0)^2 (p_0/14.7)^{2/3} W^{1/3}$; $t = t_1 (1117/c_0)(14.7 W/p_0)^{1/3}$;

and $v = v_1 (c_0/1117)$
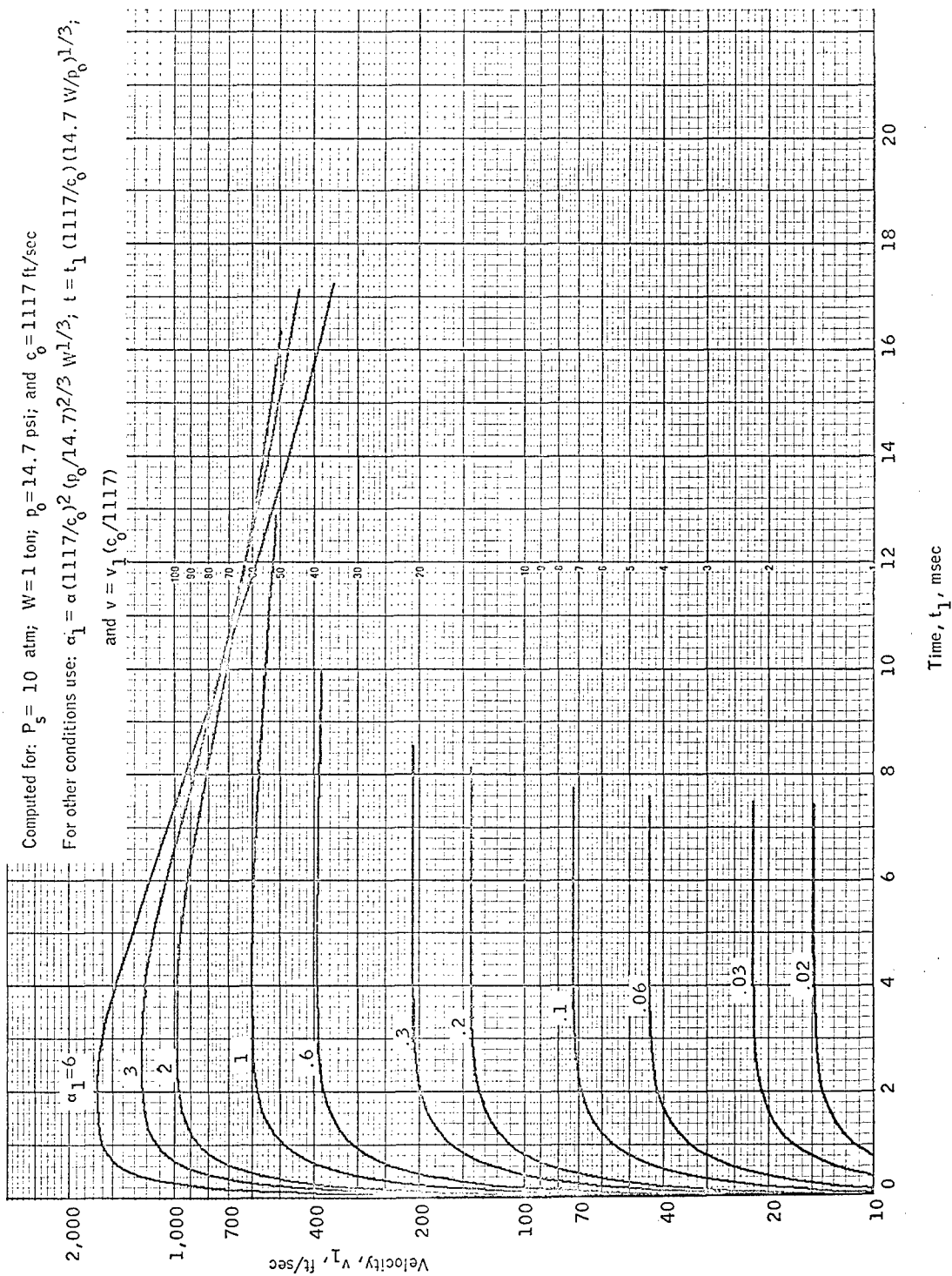
Fig. 3.19   Velocity vs. Time for $P_s = 10.0$ atm

33

Computed for: $P_s = 10$ atm; $W = 1$ ton; $p_o = 14.7$ psi; and $c_o = 1117$ ft/sec

For other conditions use: $a_1 = a (1117/c_o)^2 (p_o/14.7)^{2/3} W^{1/3}$; $t = t_1 (1117/c_o)(14.7 W/p_o)^{1/3}$;

and $d = d_1 (14.7 W/p_o)^{1/3}$

Time, $t_1$, msec

Distance, $d_1$, ft
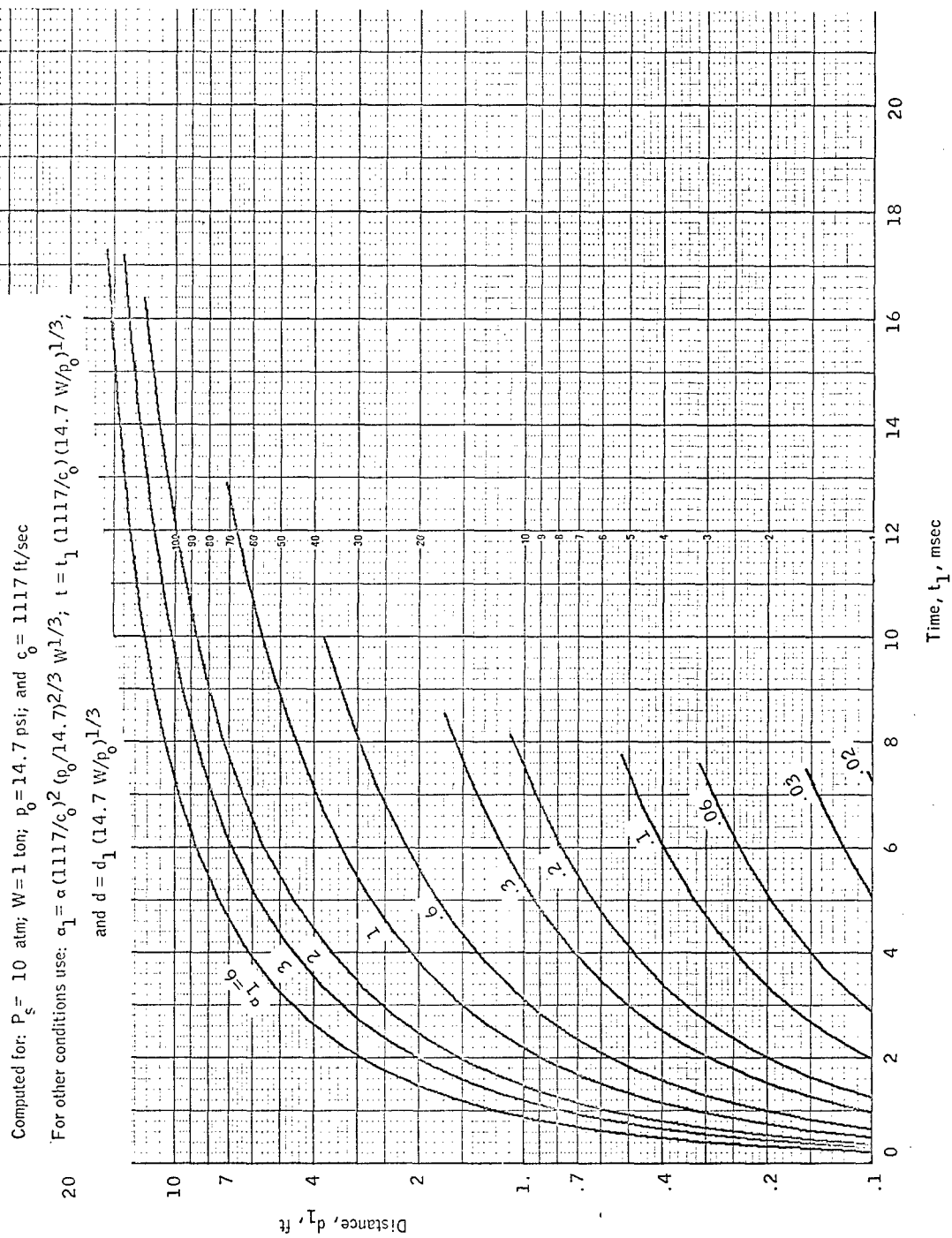
Fig. 3.20   Distance vs. Time for $P_s = 10.0$ atm

34

Computed for: $P_s = 15$ atm; $W = 1$ ton; $p_o = 14.7$ psi; and $c_o = 1117$ ft/sec

For other conditions use: $\alpha_1 = \alpha (1117/c_o)^2 (p_o/14.7)^{2/3} W^{1/3}$; $t = t_1 (1117/c_o)(14.7 \ W/p_o)^{1/3}$;

and $v = v_1 (c_o/1117)$
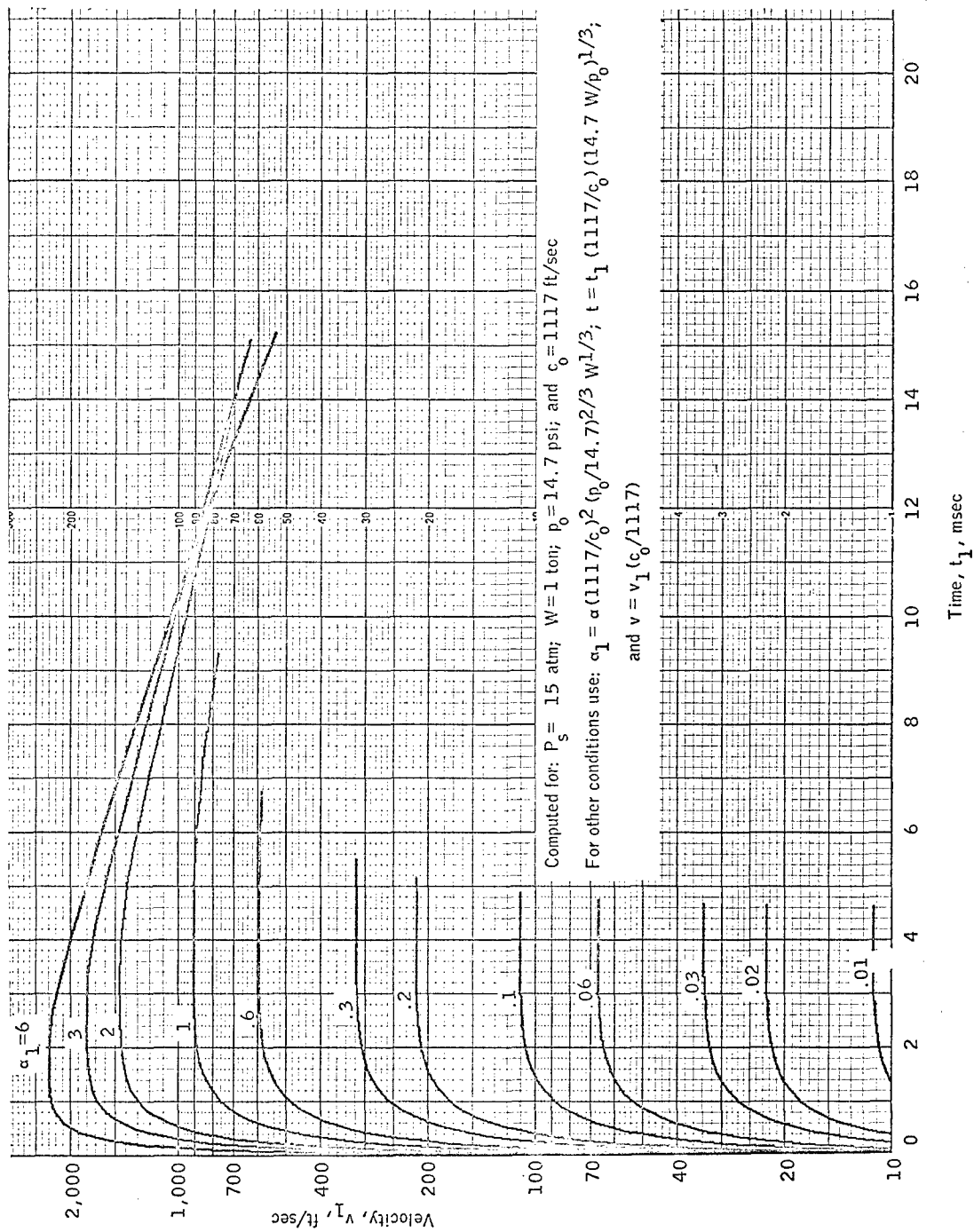
Fig. 3.21   Velocity vs. Time for $P_s = 15.0$ atm

Computed for: $P_s = 15$ atm; $W = 1$ ton; $p_o = 14.7$ psi; and $c_o = 1117$ ft/sec

For other conditions use: $\alpha_1 = \alpha \, (1117/c_o)^2 \, (p_o/14.7)^{2/3} \, W^{1/3}$; $t = t_1 \, (1117/c_o) \, (14.7 \, W/p_o)^{1/3}$;

and $d = d_1 \, (14.7 \, W/p_o)^{1/3}$

Time, $t_1$, msec

Distance, $d_1$, ft
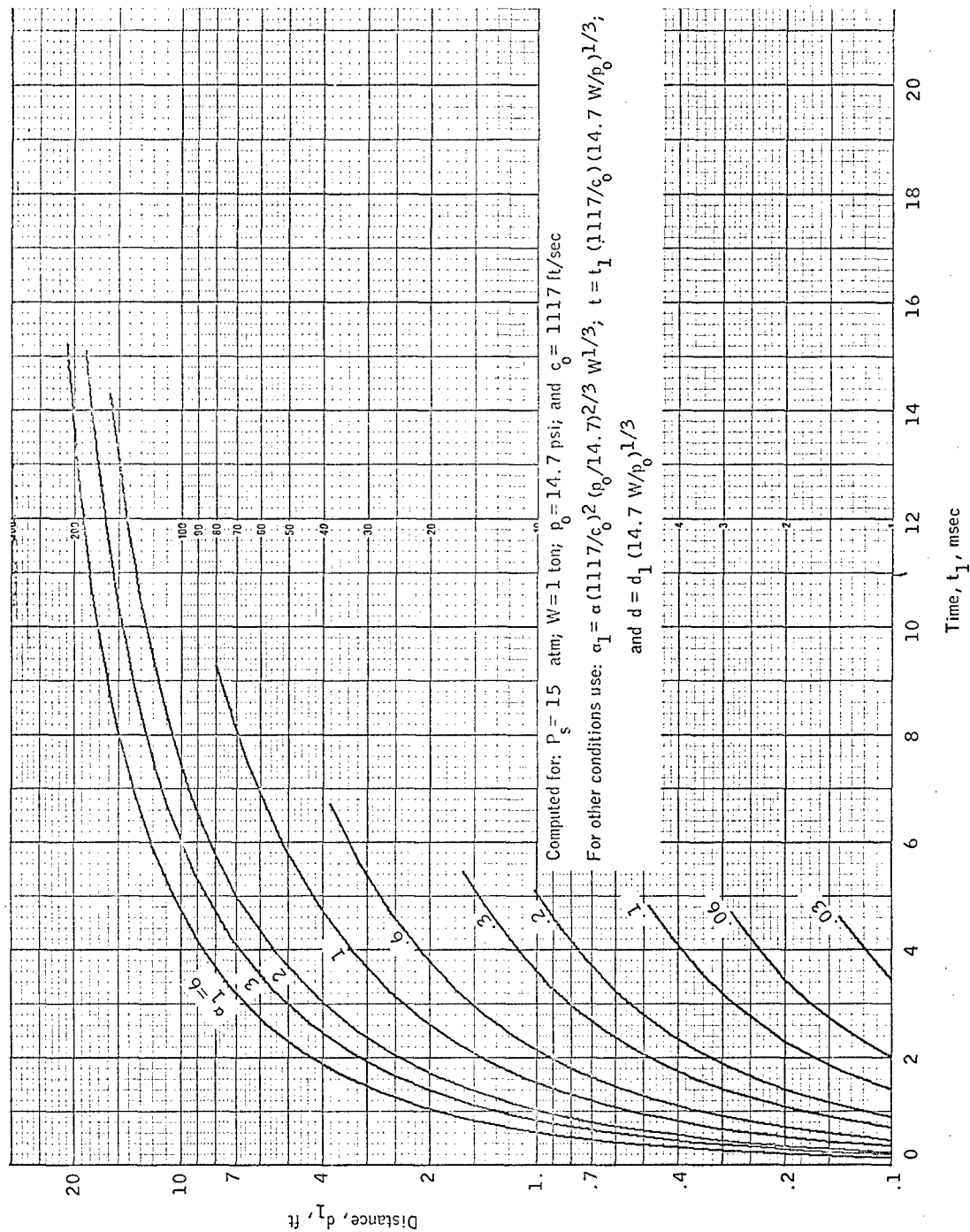
Fig. 3.22   Distance vs. Time for $P_s = 15.0$ atm

36
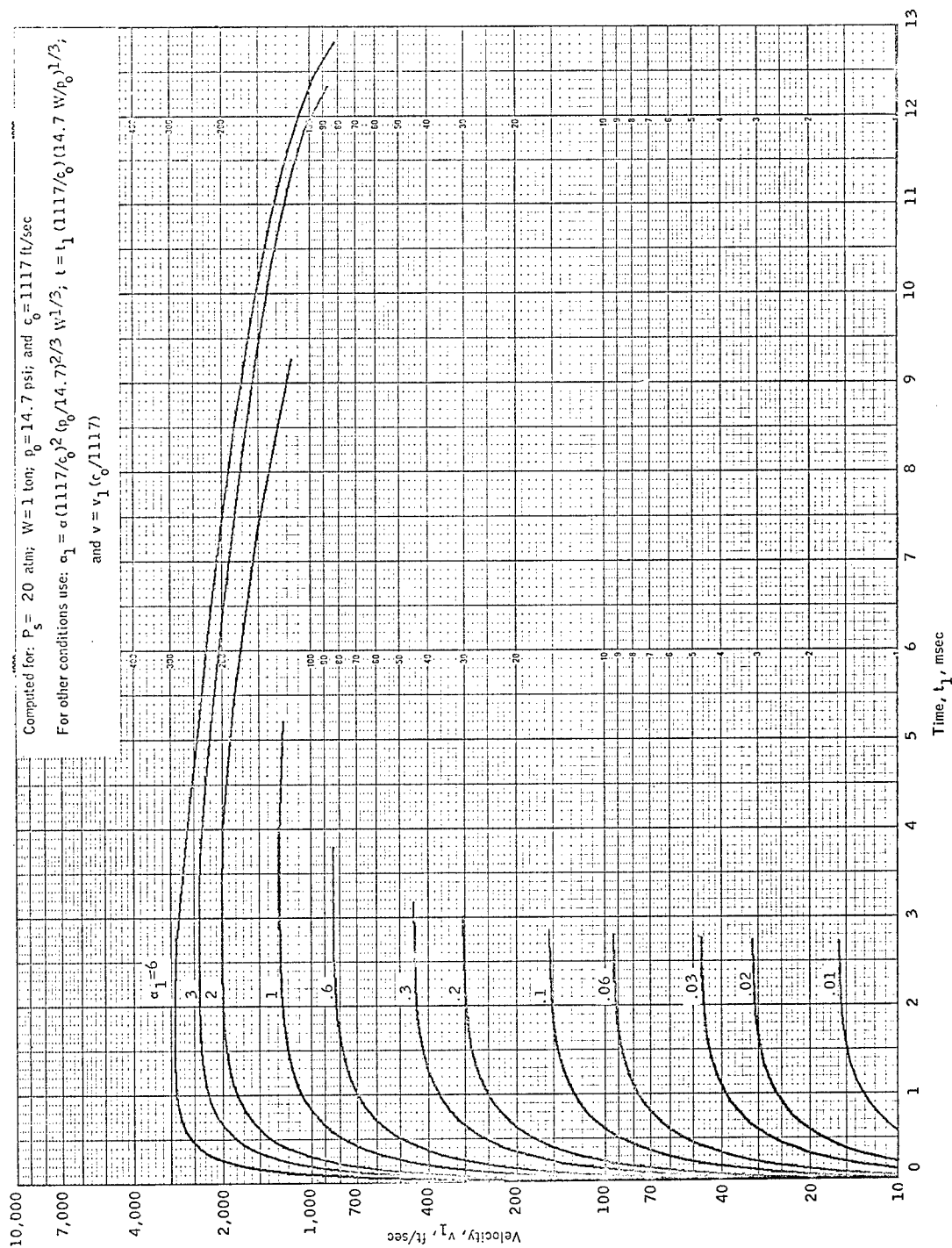
Fig. 3.23   Velocity vs. Time for $P_s$ = 20.0 atm

Computed for: $P_s$ = 20 atm;  W = 1 ton;  $p_0$ = 14.7 psi; and  $c_0$ = 1117 ft/sec

For other conditions use: $\alpha_1 = \alpha (1117/c_0)^2 (p_0/14.7)^{2/3} W^{1/3}$;  $t = t_1 (1117/c_0)(14.7 \ W/p_0)^{1/3}$;

and $v = v_1 (c_0/1117)$

Time, $t_1$, msec

Velocity, $v_1$, ft/sec

37

Computed for: $P_s = 20$ atm; $W = 1$ ton; $p_0 = 14.7$ psi; and $c_0 = 1117$ ft/sec

For other conditions use: $a_1 = a \, (1117/c_0)^2 \, (p_0/14.7)^{2/3} \, W^{1/3}$; $t = t_1 \, (1117/c_0) \, (14.7 \, W/p_0)^{1/3}$;

and $d = d_1 \, (14.7 \, W/p_0)^{1/3}$

Time, $t_1$, msec
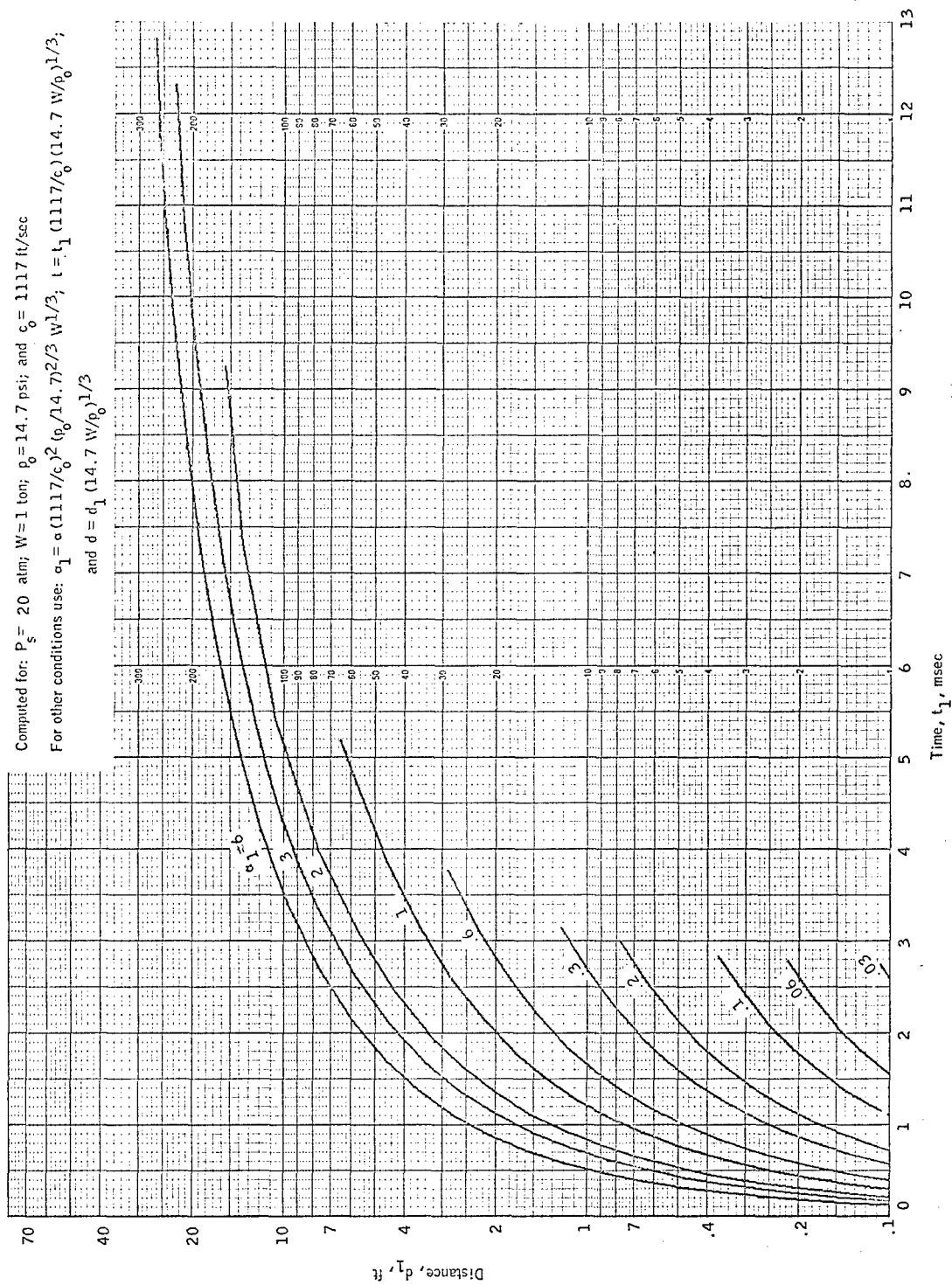
Distance, $d_1$, ft

Fig. 3.24  Distance vs. Time for $P_s = 20.0$ atm

4.0, 5.0, 6.0, 8.0, 10.0, 15.0, and 20 atms. The velocity curves for $a_1 = 6.0$, in some cases, cross those for the lower acceleration coefficients (see Fig. 3.9, for example). Comparison of the velocity charts with the blast-wave parameters shows that this phenomenon occurs only for blast waves whose dynamic pressure decays relatively fast with time; i.e., blast waves identified with the higher values of "r" listed in Table 2.2.

## 3.3 ACCELERATION VS. TIME

When a blast wave first encounters a missile having zero velocity, the maximum acceleration experienced by the missile is the product of its acceleration coefficient and the maximum dynamic pressure.* Computed values of maximum acceleration in g-units are presented in Table 3.2 for the maximum overpressures and for the acceleration coefficients used in this study. After the missile attains a finite velocity, however, missile and wind velocities also control missile acceleration.* Thus, scaling procedures are not necessary to obtain maximum acceleration, but scaling (as indicated on Figs. 3.25 to 3.36) is necessary for evaluation of accelerations occurring after the maximum.

Plots of acceleration vs. time are in Figs. 3.25 to 3.36 for the same combinations of overpressure and acceleration coefficients for which velocity and displacement data were presented in the last section. In order to separate the curves appearing on each chart, the plots were not always made to zero acceleration.

---

*This relation is expressed in Eq. (3) in Chap. 2:
$$a = q \, a \, (u - v)^2 / u^2.$$

Table 3.2

Maximum Acceleration (A, g-units) for 12 Acceleration Coefficients
($a$, ft$^2$/lb) and for 12 Maximum Overpressures (P$_s$, atm)

| P$_s$ | $a = 6$ | $a = 3$ | $a = 2$ | $a = 1$ | $a = .6$ | $a = .3$ | $a = .2$ |
|---|---|---|---|---|---|---|---|
| 1.0 | 3,970 | 1,980 | 1,320 | 662 | 397 | 198 | 132 |
| 1.5 | 8,410 | 4,200 | 2,800 | 1,400 | 841 | 420 | 280 |
| 2.0 | 14,100 | 7,060 | 4,700 | 2,350 | 1,410 | 706 | 470 |
| 2.5 | 20,900 | 10,400 | 6,960 | 3,480 | 2,090 | 1,040 | 696 |
| 3.0 | 28,600 | 14,300 | 9,530 | 4,760 | 2,860 | 1,430 | 953 |
| 4.0 | 46,200 | 23,100 | 15,400 | 7,700 | 4,620 | 2,310 | 1,540 |
| 5.0 | 66,100 | 33,100 | 22,000 | 11,000 | 6,610 | 3,310 | 2,200 |
| 6.0 | 87,900 | 44,000 | 29,300 | 14,700 | 8,790 | 4,400 | 2,930 |
| 8.0 | 135,000 | 67,700 | 45,200 | 22,600 | 13,500 | 6,770 | 4,520 |
| 10.0 | 187,000 | 93,400 | 62,300 | 31,100 | 18,700 | 9,340 | 6,230 |
| 15.0 | 325,000 | 162,000 | 108,000 | 54,100 | 32,500 | 16,200 | 10,800 |
| 20.0 | 452,000 | 226,000 | 151,000 | 75,300 | 45,200 | 22,600 | 15,100 |

| P$_s$ | $a = .1$ | $a = .06$ | $a = .03$ | $a = .02$ | $a = .01$ |
|---|---|---|---|---|---|
| 1.0 | 66.2 | 39.7 | 19.8 | 13.2 | 6.62 |
| 1.5 | 140 | 84.1 | 42.0 | 28.0 | 14.0 |
| 2.0 | 235 | 141 | 70.6 | 47.0 | 23.5 |
| 2.5 | 348 | 209 | 104 | 69.6 | 34.8 |
| 3.0 | 476 | 286 | 143 | 95.3 | 47.6 |
| 4.0 | 770 | 462 | 231 | 154 | 77.0 |
| 5.0 | 1,100 | 661 | 331 | 220 | 110 |
| 6.0 | 1,470 | 879 | 440 | 293 | 147 |
| 8.0 | 2,260 | 1,350 | 677 | 452 | 276 |
| 10.0 | 3,110 | 1,870 | 934 | 623 | 311 |
| 15.0 | 5,410 | 3,250 | 1,620 | 1,080 | 541 |
| 20.0 | 7,530 | 4,520 | 2,260 | 1,510 | 753 |

Computed for: $P_s = 1.0$ atm; $W = 1$ ton; $p_0 = 14.7$ psi; and $c_0 = 1117$ ft/sec

For other conditions use: $\alpha_1 = \alpha \ (1117/c_0)^2 \ (p_0/14.7)^{2/3} \ W^{1/3}$; $t = t_1 \ (1117/c_0) \ (14.7 \ W/p_0)^{1/3}$;

and $A = A_1 \ (c_0/1117)^2 \ (1/W)^{1/3} \ (p_0/14.7)^{1/3}$

$\alpha_1 = 6$

Acceleration, $A_1$, g-units x $10^{-2}$

Time, $t_1$, msec
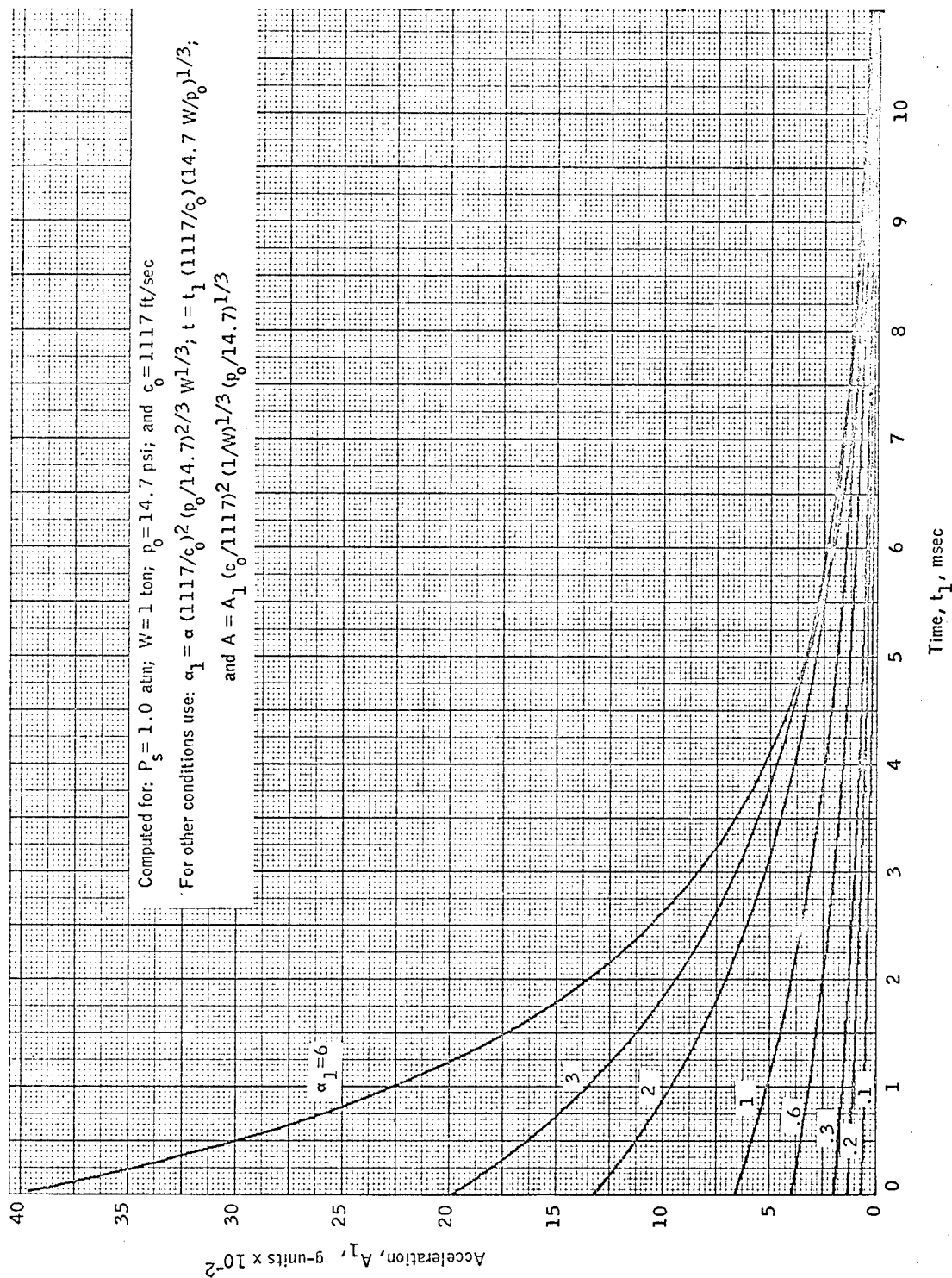
Fig. 3.25   Acceleration vs. Time for $P_s = 1.0$ atm

41

Computed for: $P_s = 1.5$ atm; $W = 1$ ton; $p_o = 14.7$ psi; and $c_o = 1117$ ft/sec

For other conditions use: $a_1 = \alpha \, (1117/c_o)^2 \, (p_o/14.7)^{2/3} \, W^{1/3}$; $t = t_1 \, (1117/c_o) \, (14.7 \, W/p_o)^{1/3}$;

and $A = A_1 \, (c_o/1117)^2 \, (1/W)^{1/3} \, (p_o/14.7)^{1/3}$
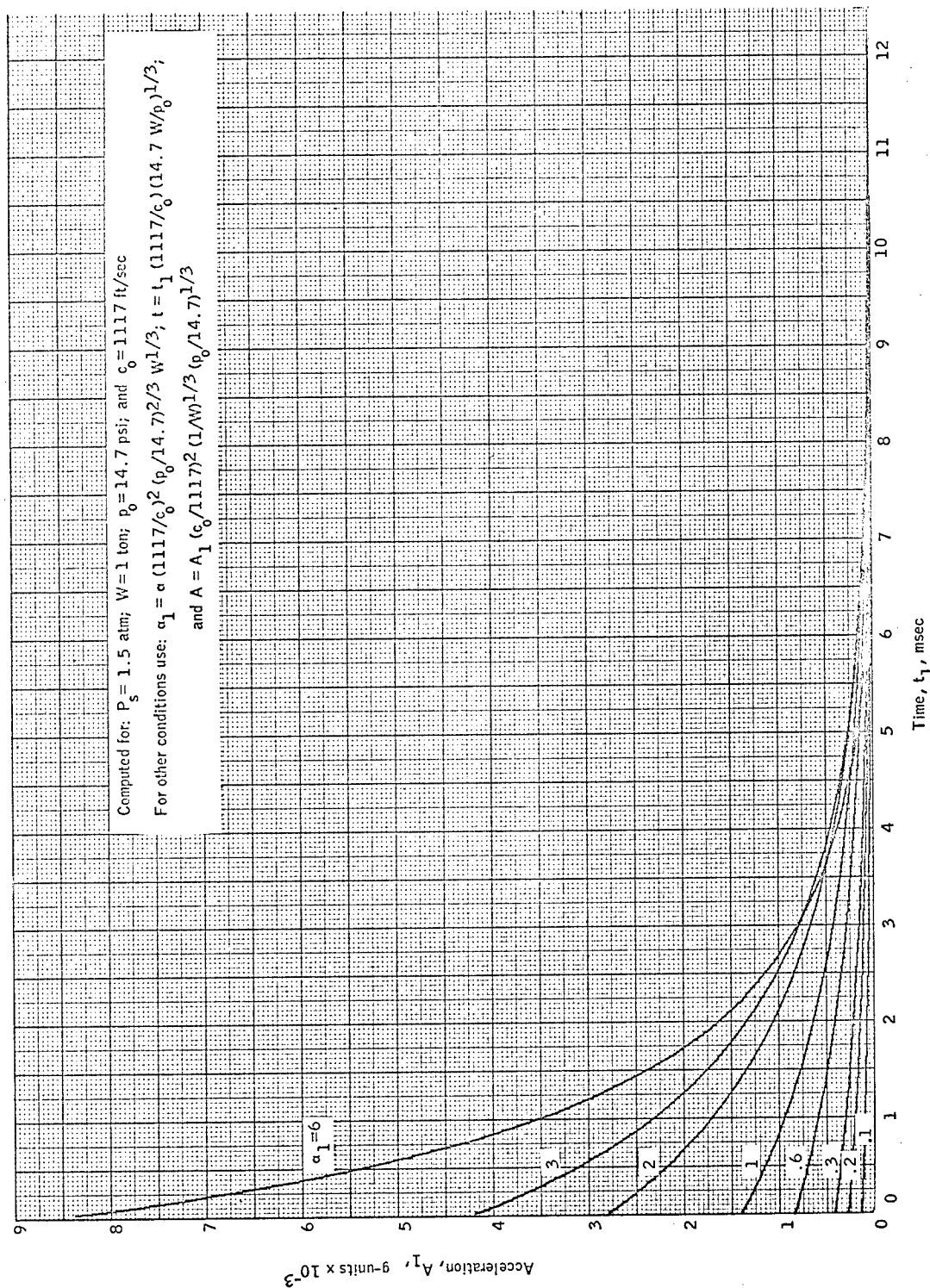
Fig. 3.26  Acceleration vs. Time for $P_s = 1.5$ atm

42

Computed for: $P_s = 2.0$ atm; $W = 1$ ton; $p_o = 14.7$ psi; and $c_o = 1117$ ft/sec

For other conditions use: $\alpha_1 = \alpha (1117/c_o)^2 (p_o/14.7)^{2/3} W^{1/3}$; $t = t_1 (1117/c_o)(14.7 W/p_o)^{1/3}$;

and $A = A_1 (c_o/1117)^2 (1/W)^{1/3} (p_o/14.7)^{1/3}$

$\alpha_1 = 6$

Acceleration, $A_1$, g-units $\times 10^{-3}$

Time, $t_1$, msec
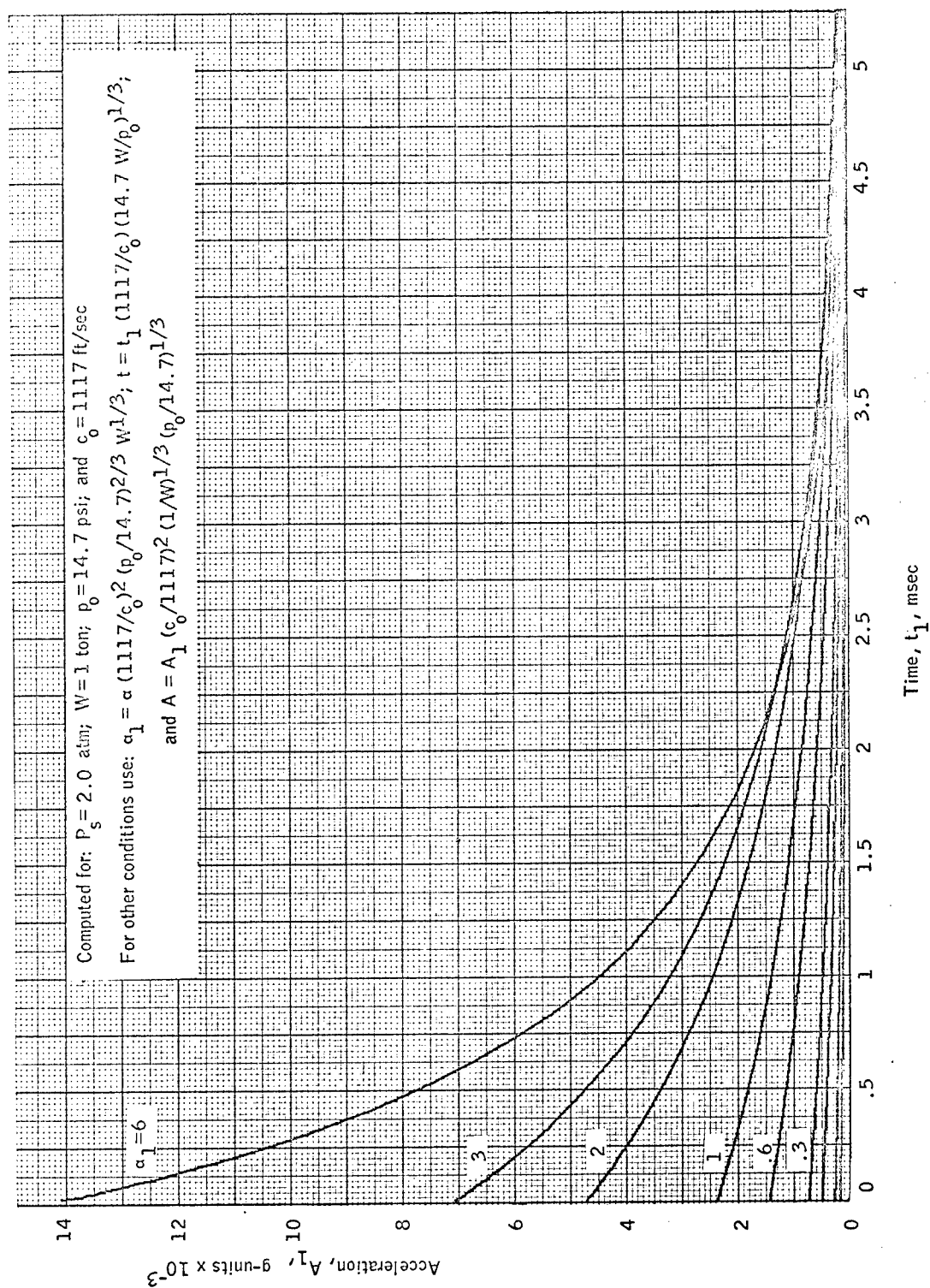
Fig. 3.27   Acceleration vs. Time for $P_s = 2.0$ atm

43

Computed for: $P_s = 2.5$ atm; $W = 1$ ton; $p_0 = 14.7$ psi; and $c_0 = 1117$ ft/sec

For other conditions use: $\alpha_1 = \alpha (1117/c_0)^2 (p_0/14.7)^{2/3} W^{1/3}$; $t = t_1 (1117/c_0) (14.7 \, W/p_0)^{1/3}$;

and $A = A_1 (c_0/1117)^2 (1/W)^{1/3} (p_0/14.7)^{1/3}$
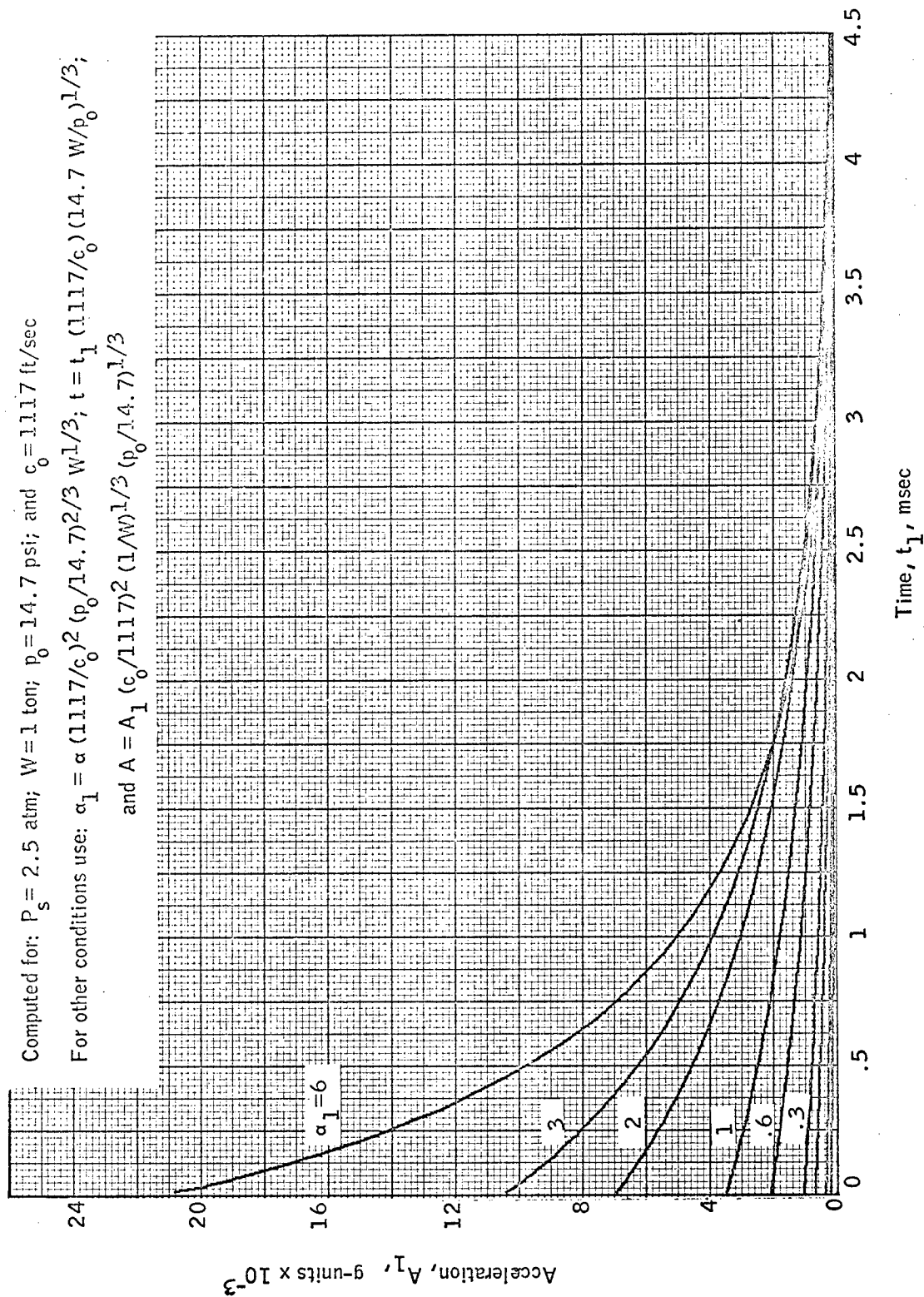
Fig. 3.28   Acceleration vs. Time for $P_s = 2.5$ atm

Computed for: $P_s = 3.0$ atm; $W = 1$ ton; $p_o = 14.7$ psi; and $c_o = 1117$ ft/sec

For other conditions use: $\alpha_1 = \alpha (1117/c_o)^2 (p_o/14.7)^{2/3} W^{1/3}$; $t = t_1 (1117/c_o)(14.7 W/p_o)^{1/3}$;

and $A = A_1 (c_o/1117)^2 (1/W)^{1/3} (p_o/14.7)^{1/3}$
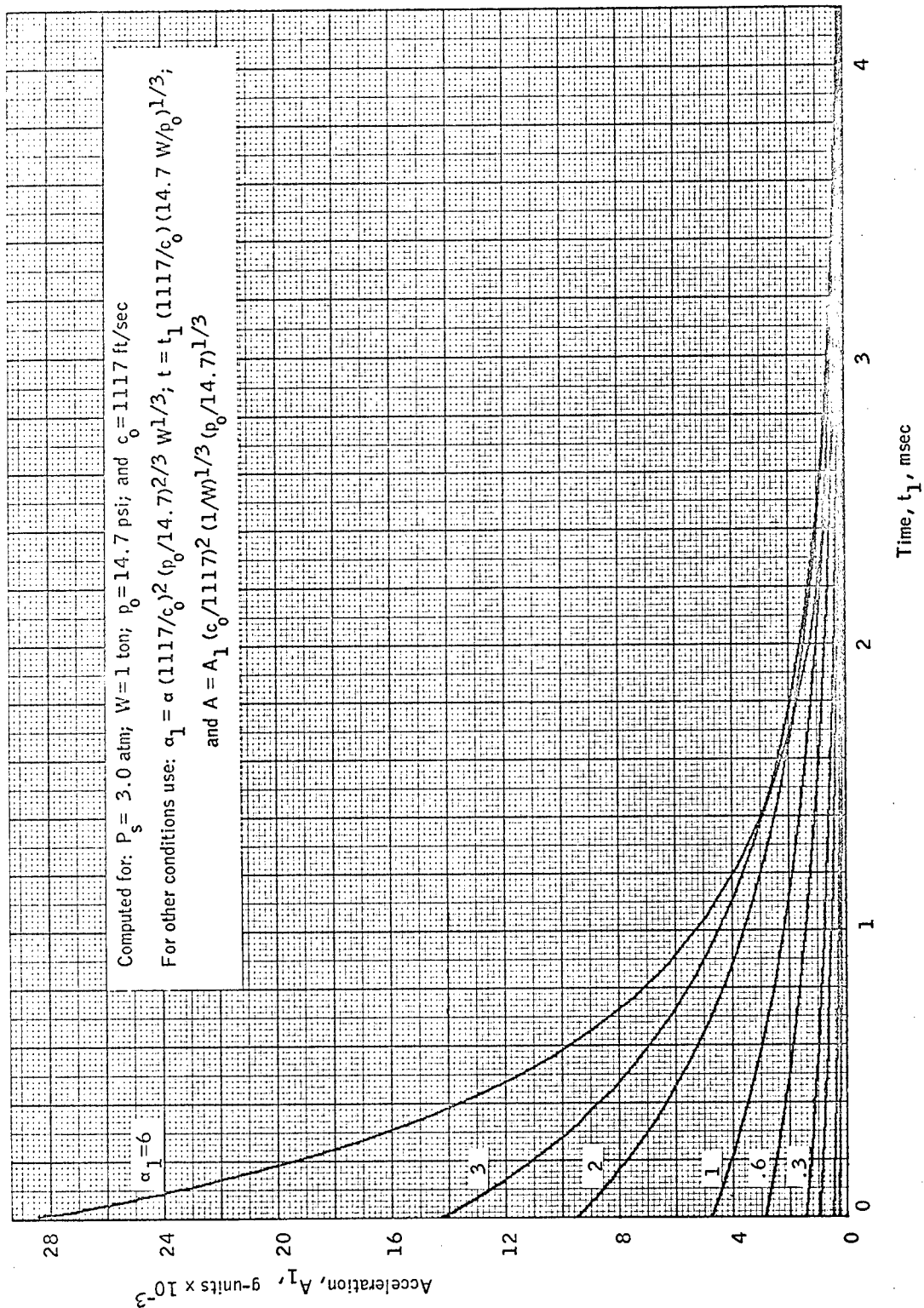
Fig. 3.29 Acceleration vs. Time for $P_s = 3.0$ atm

Computed for: $P_s = 4.0$ atm; $W = 1$ ton; $p_o = 14.7$ psi; and $c_o = 1117$ ft/sec

For other conditions use: $\alpha_1 = \alpha \, (1117/c_o)^2 \, (p_o/14.7)^{2/3} \, W^{1/3}$; $t = t_1 \, (1117/c_o) \, (14.7 \, W/p_o)^{1/3}$;

and $A = A_1 \, (c_o/1117)^2 \, (1/W)^{1/3} \, (p_o/14.7)^{1/3}$
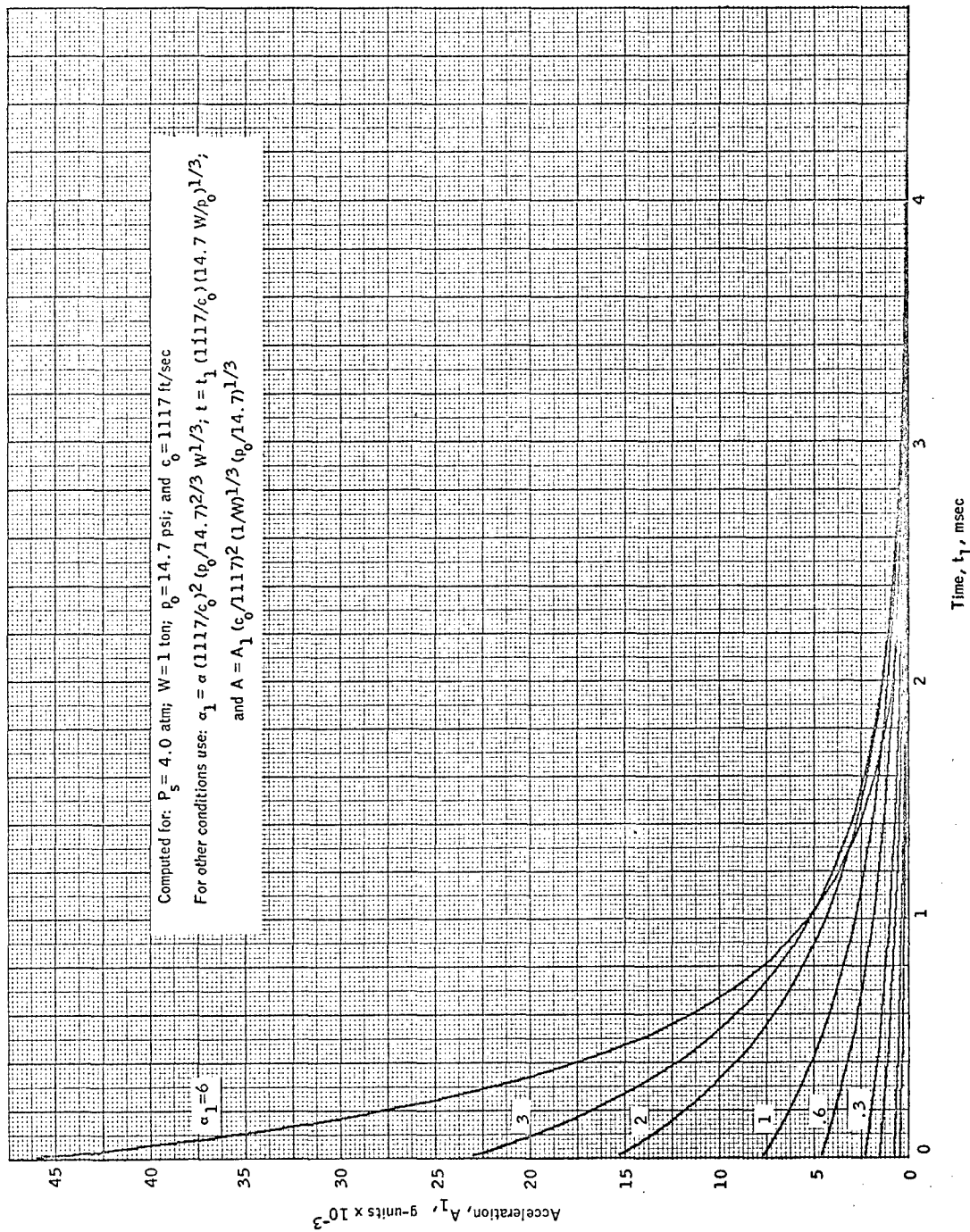
Fig. 3.30   Acceleration vs. Time for $P_s = 4.0$ atm

46

Computed for: $P_s = 5.0$ atm; $W = 1$ ton; $p_o = 14.7$ psi; and $c_o = 1117$ ft/sec

For other conditions use: $a_1 = a (1117/c_o)^2 (p_o/14.7)^{2/3} W^{1/3}$; $t = t_1 (1117/c_o) (14.7 W/p_o)^{1/3}$;

and $A = A_1 (c_o/1117)^2 (1/W)^{1/3} (p_o/14.7)^{1/3}$
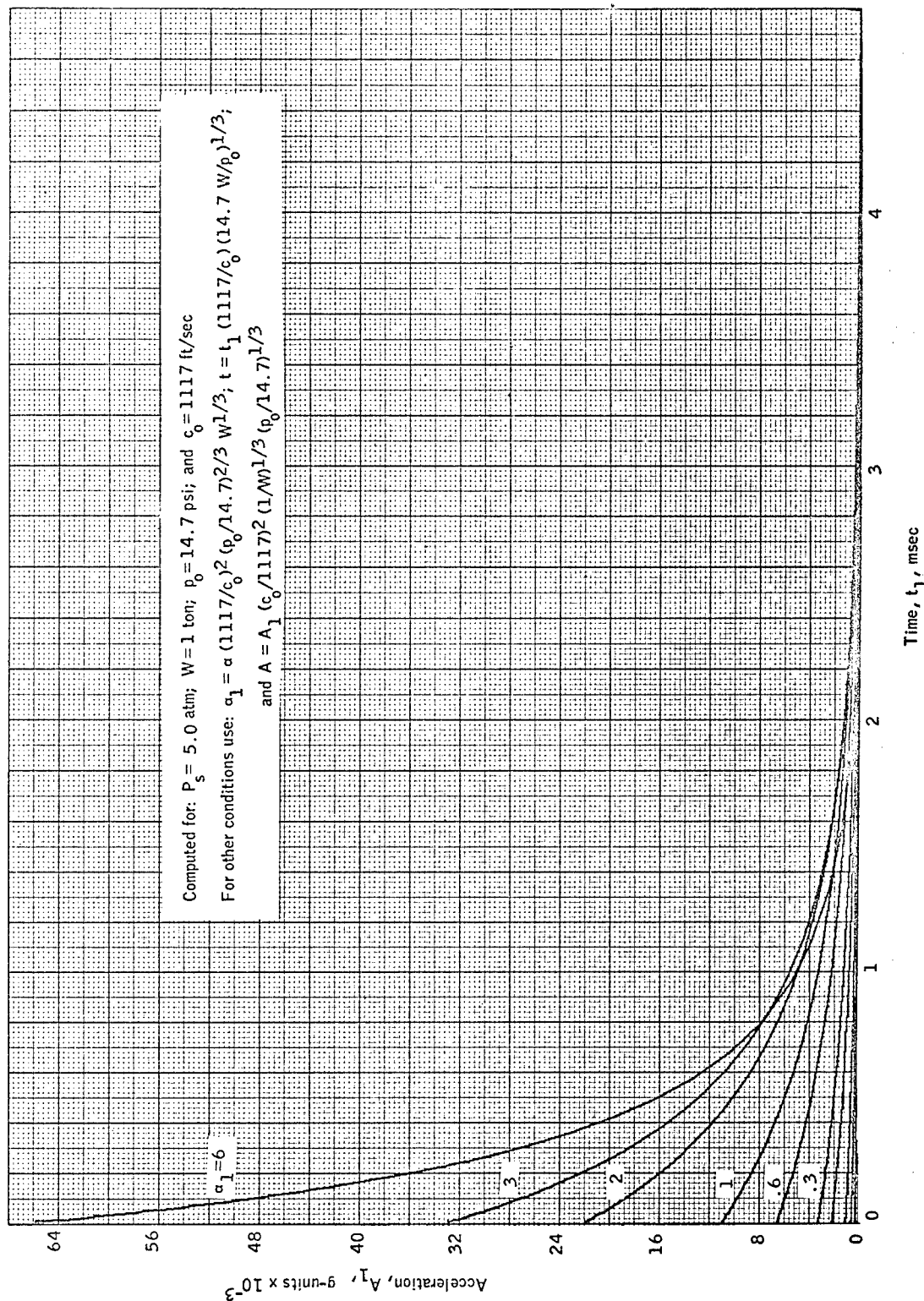
Fig. 3.31   Acceleration vs. Time for $P_s = 5.0$ atm

Time, $t_1$, msec

Acceleration, $A_1$, g-units x $10^{-3}$

Computed for: $P_s = 6.0$ atm; $W = 1$ ton; $p_o = 14.7$ psi; and $c_o = 1117$ ft/sec

For other conditions use: $a_1 = a (1117/c_o)^2 (p_o/14.7)^{2/3} W^{1/3}$; $t = t_1 (1117/c_o)(14.7 W/p_o)^{1/3}$;

and $A = A_1 (c_o/1117)^2 (1/W)^{1/3} (p_o/14.7)^{1/3}$

$a_1 = 6$

3

2

1

.6

Acceleration, $A_1$, g-units x $10^{-4}$

Time $t_1$, msec
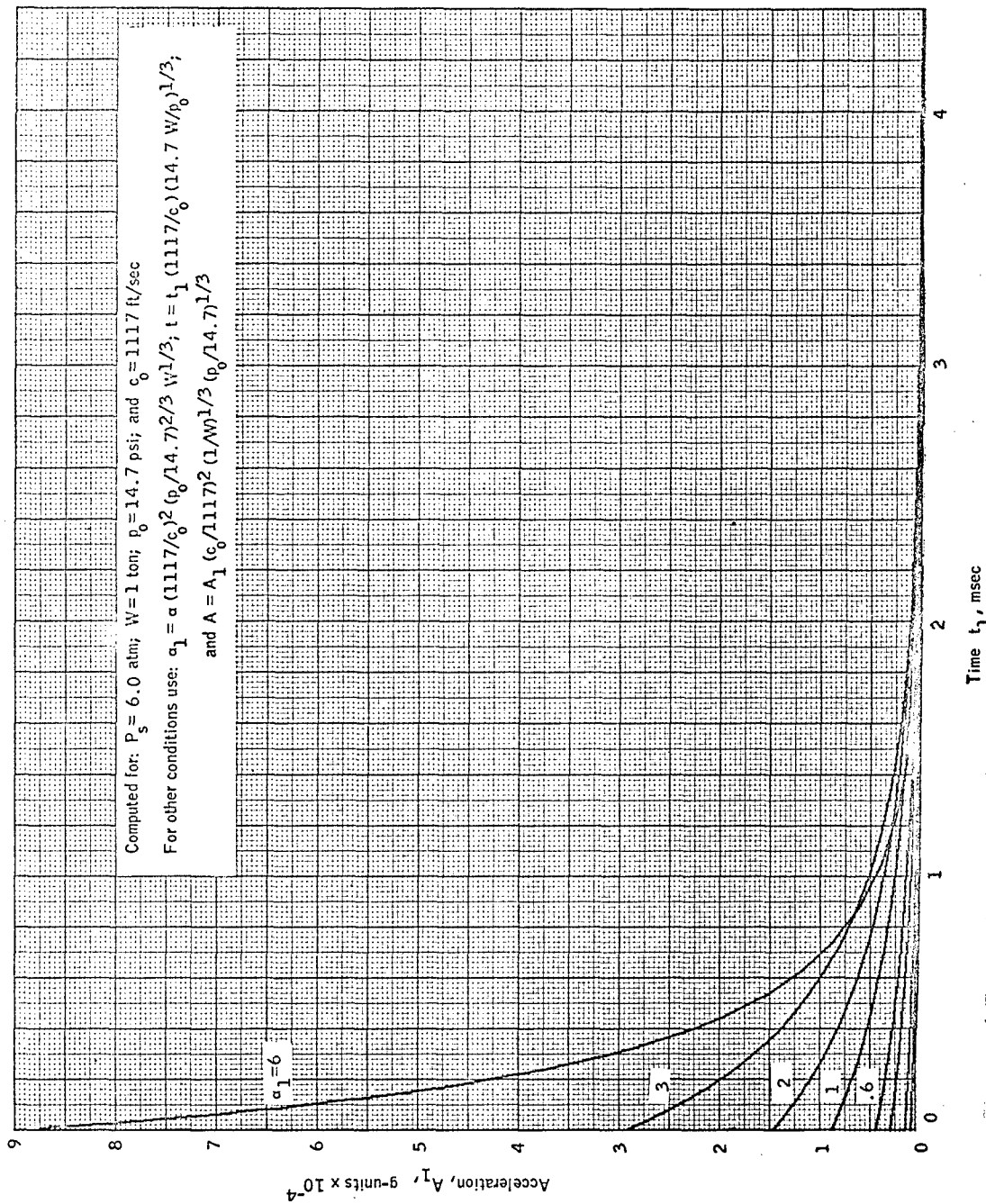
Fig. 3.32   Acceleration vs. Time for $P_s = 6.0$ atm

48

Computed for: $P_s = 8.0$ atm; $W = 1$ ton; $p_o = 14.7$ psi; and $c_o = 1117$ ft/sec

For other conditions use: $\alpha_1 = \alpha \, (1117/c_o)^2 \, (p_o/14.7)^{2/3} \, W^{1/3}$; $t = t_1 \, (1117/c_o) \, (14.7 \, W/p_o)^{1/3}$;

and $A = A_1 \, (c_o/1117)^2 \, (1/W)^{1/3} \, (p_o/14.7)^{1/3}$

$\alpha_1 = 6$

3

2

1

.6

.3
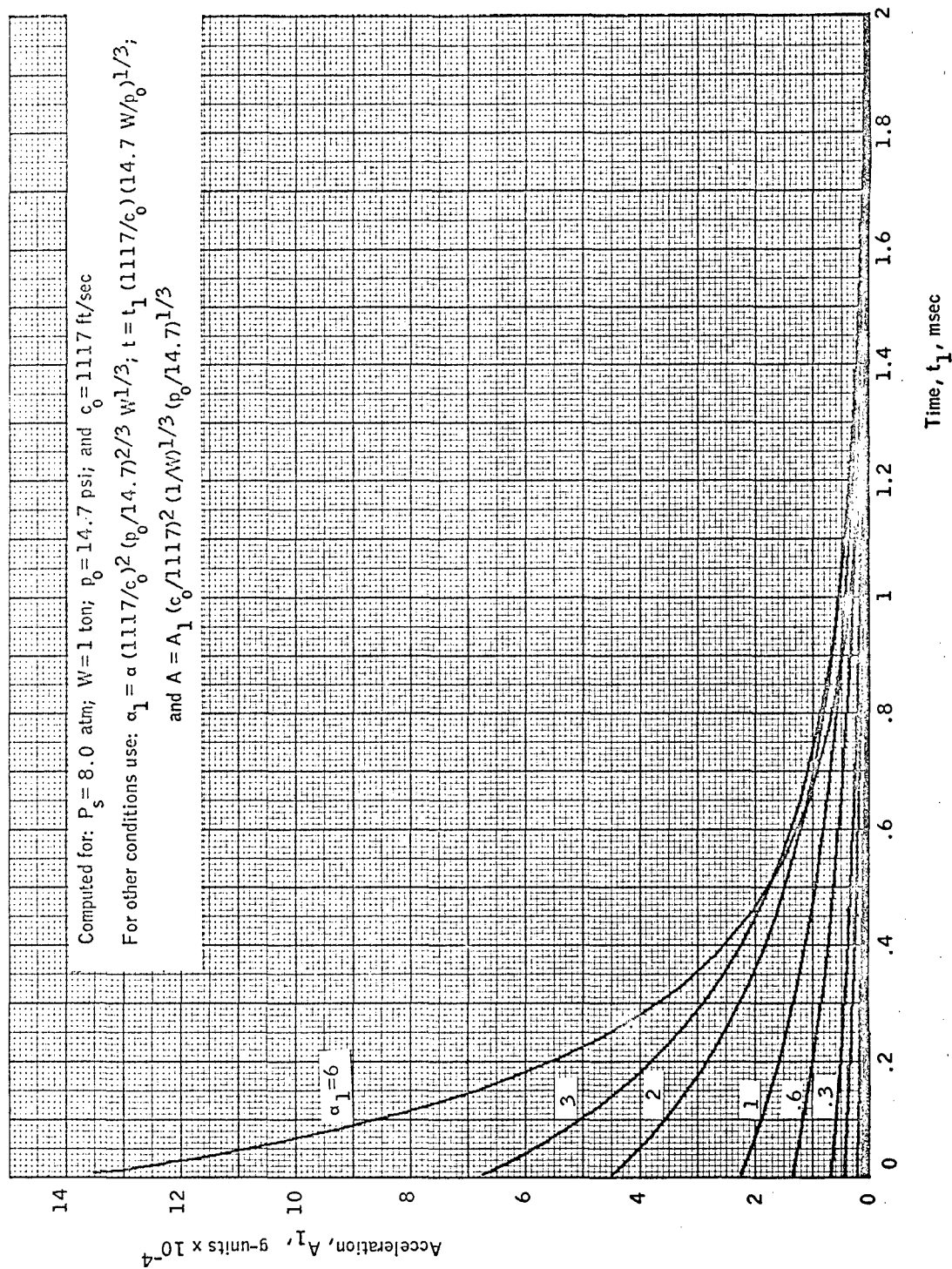
Fig. 3.33   Acceleration vs. Time for $P_s = 8.0$ atm

Computed for: $P_s = 10$ atm; $W = 1$ ton; $p_0 = 14.7$ psi; and $c_0 = 1117$ ft/sec

For other conditions use: $a_1 = a \ (1117/c_0)^2 \ (p_0/14.7)^{2/3} \ W^{1/3}$, $t = t_1 \ (1117/c_0) \ (14.7 \ W/p_0)^{1/3}$;

and $A = A_1 \ (c_0/1117)^2 \ (1/W)^{1/3} \ (p_0/14.7)^{1/3}$
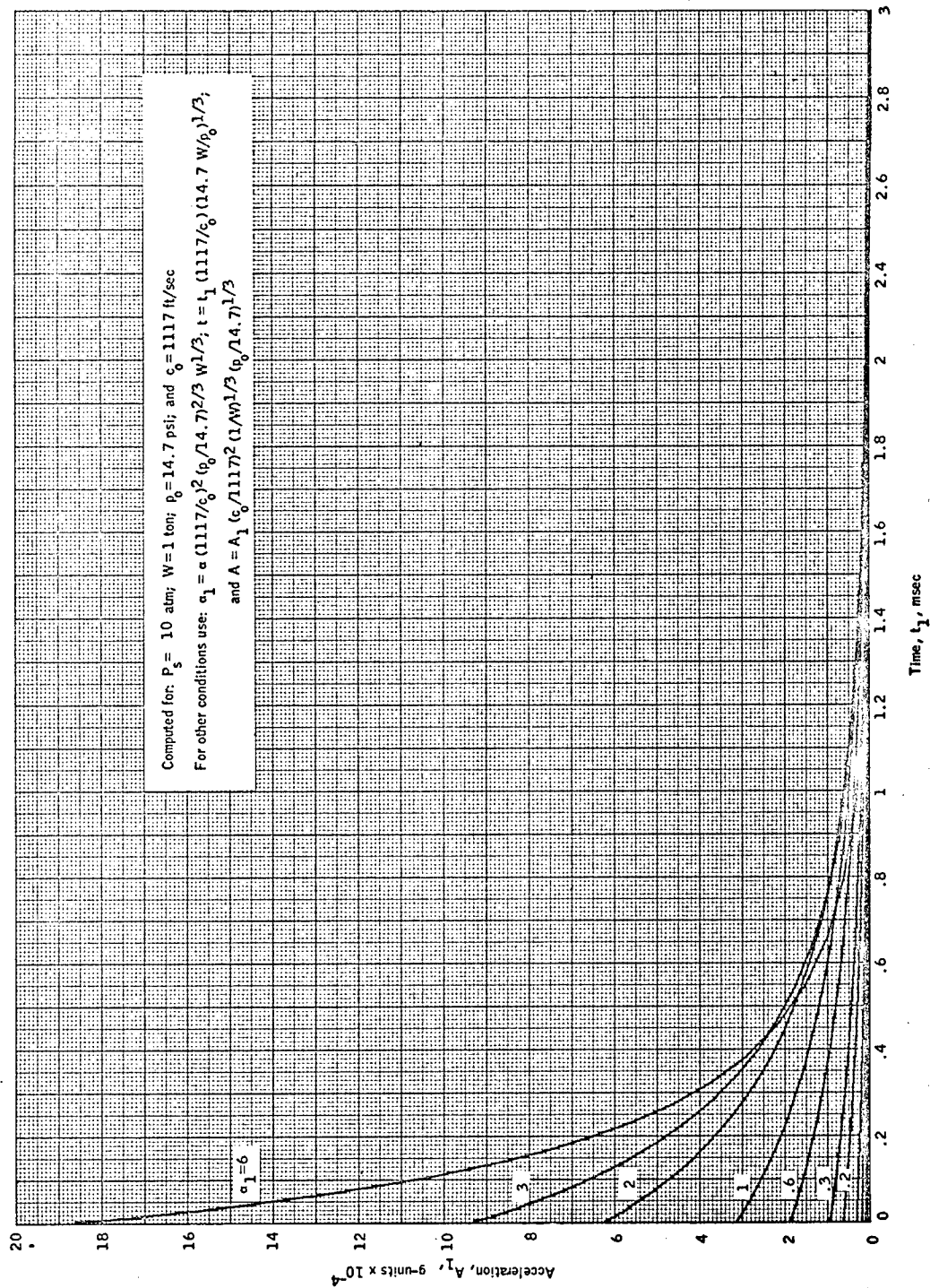
Fig. 3.34  Acceleration vs. Time for $P_s = 10.0$ atm
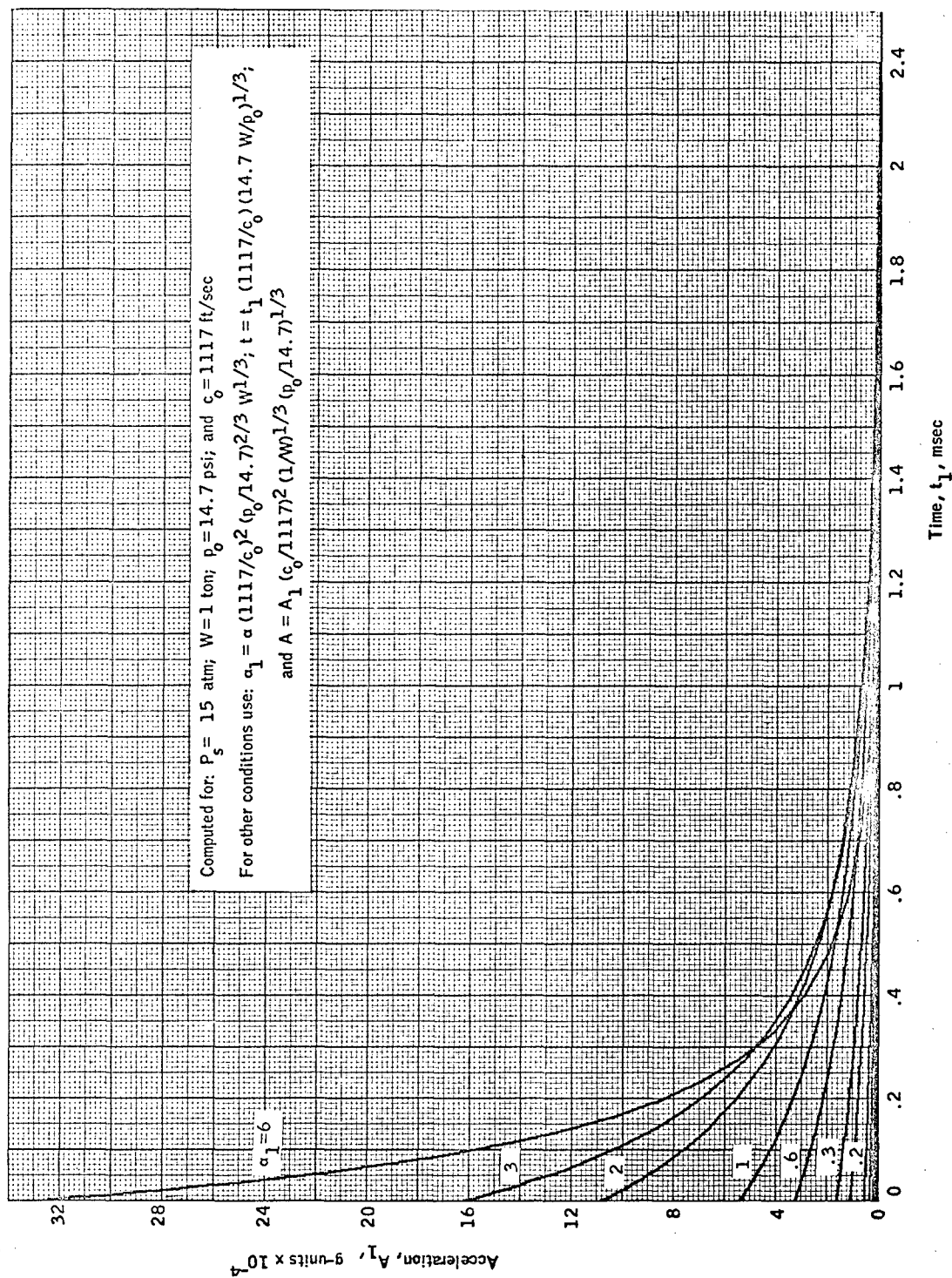
Fig. 3.35    Acceleration vs. Time for $P_s$ = 15.0 atm

The chart contains the following annotations:

Computed for: $P_s$ = 15 atm; W = 1 ton; $p_0$ = 14.7 psi; and $c_0$ = 1117 ft/sec

For other conditions use: $\alpha_1 = \alpha (1117/c_0)^2 (p_0/14.7)^{2/3} W^{1/3}$; $t = t_1 (1117/c_0)(14.7 W/p_0)^{1/3}$;

and $A = A_1 (c_0/1117)^2 (1/W)^{1/3} (p_0/14.7)^{1/3}$

Vertical axis: Acceleration, $A_1$, g-units × $10^{-4}$

Horizontal axis: Time, $t_1$, msec

Curve labels: $\alpha_1 = 6$, 3, 2, 1, .6, .3, .2

Computed for: $P_s = 20$ atm; $W = 1$ ton; $p_o = 14.7$ psi; and $c_o = 1117$ ft/sec

For other conditions use: $a_1 = a (1117/c_o)^2 (p_o/14.7)^{2/3} W^{1/3}$, $t = t_1 (1117/c_o) (14.7 W/p_o)^{1/3}$,

and $A = A_1 (c_o/1117)^2 (1/W)^{1/3} (p_o/14.7)^{1/3}$

Time, $t_1$, msec

Fig. 3.36   Acceleration vs. Time for $P_s = 20.0$ atm

52

REFERENCES   CHAPTER 3

1.  Bowen, I. G., R. W. Albright, E. R. Fletcher and
    C. S. White, A Model Designed to Predict the Motion
    of Objects Translated by Classical Blast Waves, Civil
    Effects Test Operations, USAEC Report CEX-58.9,
    June 29, 1961.

2.  Fletcher, E. R., R. W. Albright, V. C. Goldizen and
    I. G. Bowen, Determinations of Aerodynamic-Drag
    Parameters of Small Irregular Objects by Means of
    Drop Tests, Civil Effects Test Operations, USAEC Report
    CEX-59.14, October, 1961.

# CHAPTER 4  DISCUSSION

## 4. 1  MODEL RELIABILITY

This report presents numerical predictions of the behavior of objects set in motion by high-explosive blast waves. Unfortunately, these predictions cannot be compared with experimental data. The translation model,[1] however, has been successfully used to predict the results of secondary-missile experiments made at the Nevada Test Site with nuclear-produced blast waves which were near ideal (or classical) in character.* In another experiment with anthropomorphic dummies[1,3], maximal velocity could be successfully computed using an average acceleration coefficient for a tumbling dummy. However, to duplicate more precisely the velocity-distance measurements, it was necessary to use an acceleration coefficient which was a function of the orientation of the dummy during translation.

## 4. 2  COMPARISON WITH NUCLEAR TRANSLATIONAL EFFECTS

In comparison with results computed for nuclear blast waves, those for high-explosive waves indicate that the overpressure must be considerably higher for an object to attain the same maximum velocity. This velocity occurs, however, after a much shorter distance of translation. Because of the short distances involved, it seems reasonable, in many cases, to assume that a translated man would not change orientation during the accelerative phase of displacement induced by high explosives; thus, a nonvarying acceleration coefficient corresponding to that of his original posture could be used. For example, the charts in Fig. 3. 13 and 3. 14 for $P_s$ = 5 atm and W = 1 ton show that a standing person with an acceleration coefficient of 0. 06 $ft^2$/lb would attain a velocity of 23 ft/sec in only 0. 1 ft of travel.

A comparison was made in Sect. 3. 2 between the velocities predicted using nuclear and high-explosive blast data evaluated for the conditions: $P_s$ = 1 atm, W = 1 kt, $P_o$ = 14. 7 psi, $c_o$ = 1117 ft/sec.

---

*In these experiments, reported in Ref. 2, the velocities were measured for stones and spheres in open areas and for glass fragments from windows facing the oncoming blast wave. The blast wave entering the houses through the windows was modified; however, if it was assumed to have a maximum overpressure equal to the reflected value of normal incidence, the maximum fragment velocities could be predicted.

For high acceleration coefficients the velocities were in reasonable agreement, but not for low coefficients. This discrepancy results from differences in the blast parameters specified for the two types of blast waves and serves to emphasize the importance of input data in determining the computed results. One method for verifying the input data, as well as the model used in the present study, is to perform field experiments similar to those done with nuclear explosions.[2,3]

## 4.3  BIOMEDICAL INTERESTS

### 4.3.1  General

Those interested in the relation between environmental medicine and weapons effects recognize that any reasonably complete understanding of the many problems envolved requires information in the physical, biophysical and biomedical areas. In this regard, a conceptual guide for analytical procedures and research planning is essential; indeed such has been proposed[4] wherein five problem areas were defined to elucidate the kinds of data needed to establish a quantitative fabric that would allow the source of an environmental variation to be "tied" to hazards assessment.

The five problem areas, plus another concerned with bio-medical tasks, are listed in Table 4.1. The first three — encompassing "free-field" scaling, "geometric" scaling and secondary events — represent ground that must be "spaded" mostly by those qualified in the physical sciences if understanding of the environmental variations that can occur at potentially populated locations is to be forthcoming.

Contemplation of the remaining three problem areas make it apparent that hazards assessment requires knowledge of biologic response and the etiologic mechanisms involved. Such knowledge, in turn, touches biomedical tasks such as therapy, rehabilitation and all possible means for minimizing casualties through whatever protective measures might prove effective and feasible. It is here that personnel qualified in biophysics, biology and medicine can contribute.

### 4.3.2  The Translational Problem

#### Missiles

Since experience has shown that blast-induced environmental variations which are potentially hazardous include the translation of both animate and inanimate objects, applicable and definitive

Table 4.1

Problem Areas Relevant to Biologic
Effects of Nuclear Weapons

| | | |
|---|---|---|
| Source | Design Yield Burst conditions Range Weather | "Free-field" scaling* |
| Attenuation and Augmentation | Modification of "free-field" phenomena by geometric conditions of exposure | "Geometric" scaling |
| Physical Interaction | Energy transfer to: Physical objects and biological material | Secondary events |
| Biophysical Interaction | Energy dissipation by or within biologic targets | Etiologic mechanisms |
| Biologic Response | Major medical syndromes Isolated individual effects and combined injury | Hazard assessment |
| Biomedical Tasks | Therapeutic and prophylactic measures | Casualty care Rehabilitation Protective procedures |

*See Fig. 4.1 which shows the maximal values of overpressure as a function of range from a 1 ton surface burst of high explosives at sea level. The chart is useful since it allows one to determine ranges for the overpressures mentioned in Sect. 3.1.
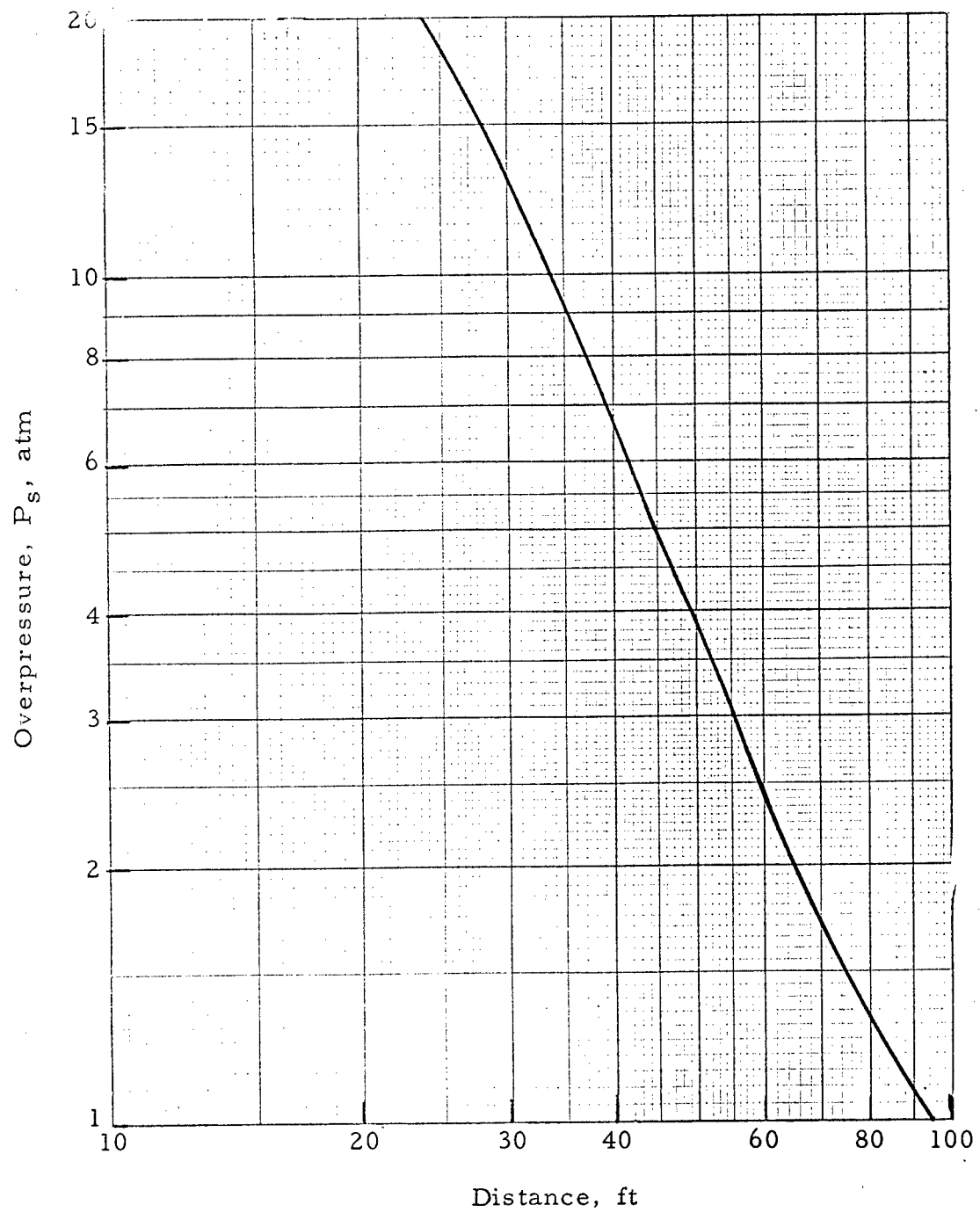
Fig. 4.1. Overpressure vs. distance from surface burst of
1 ton high explosives. (Sea-level conditions)

data are required for any comprehensive analysis. For example, among the factors that contribute to the casualty potential of blast-energized missiles are the velocity and angle of impact; the mass density, shape and character of the debris; and the area of the body receiving penetrating and/or nonpenetrating wounds.

### Displacement

Similarly, the potential for injury as a consequence of gross displacement of biological targets may be due to accelerative and/or decelerative loading. The former depends at least upon the magnitude of the forces vs. time which initiate displacement and upon the initial and subsequent orientations of the biologic target. The latter depends mostly upon the velocity at which deceleration occurs, the character of the decelerating surface and the area or areas of the body involved whether impacting with a solid object or tumbling over some near-horizontal sur- face transpires.

### 4. 3. 3 Present Study

The previous paragraphs help to place in context the con- tribution of the analytical data presented in earlier sections of this report in which physical principles were employed to estab- lish a quantitative relationship between free-field blast parameters and the aerodynamic characteristics of objects that may be dis- placed by blast winds. Thus, one may determine or estimate many of the important physical factors, and the quantitative values associ- ated therewith, that are pertinent to the assessment of environ- mental hazards.

For example, it is desirable to know what the velocity of debris may be as a function of yield, range, and distance of travel for inanimate objects having various areas, masses, and drag coefficients. Likewise, it is of value to know the order of magnitude and duration of the "G" loads imposed on animate objects by blast winds associated with different overpressures produced by various explosive yields. Also, under similar circumstances, it is helpful to have values for the velocity of animate objects as a function of time and distance of travel. The latter is often pertinent because the work space of one exposed individual may allow only a few feet of travel and thus limit the impact velocity; for another individual the environment may allow attainment of a higher and perhaps maxi- mal velocity before decelerative events occur.

Thus the graphic data prepared for the present study not only contribute to the physical aspects of blast effects, but also offer

information of value to thos interested in blast and shock biology as will be noted briefly below.

## 4.3.4  Biological Interests

There are at least two reasons why quantitative data relevant to blast-induced translation of objects interest biomedical personnel. The first is entirely pragmatic, but requires that enough information about biologic response be available to formulate biologic criteria equal to the challenge of hazards assessment. When such criteria exist, it becomes analytically possible to set forth, as functions of yield and range, "safe" areas and those within which performance may be degraded, casualties may occur, and various levels of lethality can be expected.

The second reason physical data relevant to blast-induced environmental variations intrigue blast biologists is related to the fact that biological-response data are frequently lacking or are inadequate for hazards assessment. Under such circumstances the physical information can be used to plan conceptually and to direct more realistic research programs. A case in point concerns the very high initial G-loads predicted for objects the size and shape of man set forth in Table 3.2 and the G-time patterns contained in Figs. 3.25 to 3.36 applicable to the 168-lb man; viz. , acceleration coefficient $(a)$ values of .052, .021, and .0063 for individuals standing facing the wind, crouching facing the wind, and prone aligned with the wind, respectively. The physical data strictly refer to the displacement of the center of gravity of rigid objects simulating an "average" man. They specify G-loadings that rise "instantaneously" to very high values and decay differently with time depending upon yield, range, acceleration coefficient, etc. They say nothing about the G-time variations that actually occur on the down-stream side of semi-elastic living object compared with the up-stream-side or about the associated loads applied to different internal body organs.

The physical data, however, do pose problems for perceptive biologists. For example, what is the biology of instantaneously applied G-loadings? Can high-density blast winds produce injury only because they suddenly "push" a man too fast, and if so, under what circumstances? Are the significant effects, if any, limited to small explosive charges and to "isolated" portions of the body such as fingers, feet, extremities, etc.? What is the comparative range-yield relationships between these kinds of G-loads and hazards due to primary (pressure) and secondary (missiles) blast effects?